Chemical Research in Toxicology®



Article

# 2,6-Dihydroxybenzaldehyde analogues of the iron chelator salicylaldehyde isonicotinoyl hydrazone: Increased hydrolytic stability and cytoprotective activity against oxidative stress

Hana Jansová, Jan Kubeš, Petra Reimerova, Petra Št#rbová-Kova#íková, Jaroslav Roh, and Tomas Simunek

*Chem. Res. Toxicol.*, **Just Accepted Manuscript** • DOI: 10.1021/acs.chemrestox.8b00165 • Publication Date (Web): 17 Oct 2018



ACS Publications

is published by the American Chemical Society. 1155 Sixteenth Street N.W., Washington, DC 20036

# 2,6-Dihydroxybenzaldehyde analogues of the iron chelator salicylaldehyde isonicotinoyl hydrazone: Increased hydrolytic stability and cytoprotective activity against oxidative stress

*Hana Jansová, Jan Kubeš, Petra Reimerová, Petra Štěrbová-Kovaříková, Jaroslav Roh*,*

*Tomáš Šimůnek**

Charles University, Faculty of Pharmacy in Hradec Králové, Akademika Heyrovského 1203, 500 05 Hradec Králové, Czech Republic

*Authors for correspondence:

Assoc. Prof. Jaroslav Roh
Tel.: +420-495-067-339; Fax: +420-495-067-339
E-mail: Jaroslav.Roh@faf.cuni.cz

Prof. Tomáš Šimůnek
Tel.: +420-495-067-422; Fax: +420-495-067-168
E-mail: Tomas.Simunek@faf.cuni.cz

# Table of Contents (TOC) graphic

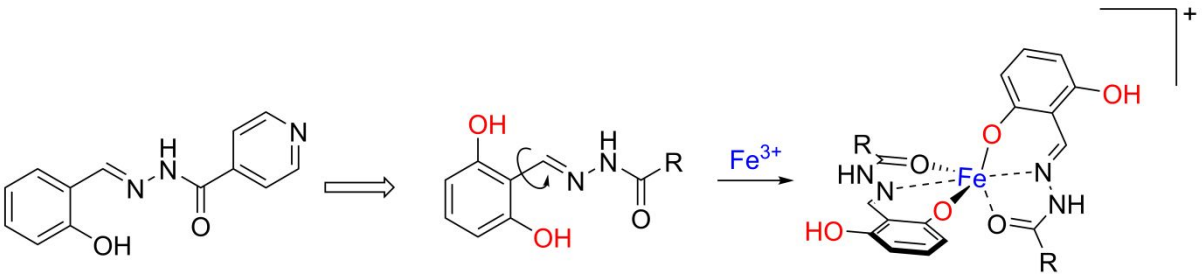


-similar chelating activity
-similar cytotoxicity
**-higher cytoprotection against oxidative stress**


# Abstract

Salicylaldehyde isonicotinoyl hydrazone (SIH) is a small molecule and lipophilic chelating agent that firmly binds ferric ions from the cellular labile iron pool, and is able to protect various tissues against oxidative damage. Previously, SIH possessed the best ratio of cytoprotective efficiency to toxicity among various iron chelators, including the desferrioxamine, deferiprone and deferasirox used in clinical practice. Here, we prepared a series of 2,6-dihydroxybenzaldehyde aroylhydrazones as SIH analogues with an additional hydroxyl group that can be involved in the chelation of metal ions. Compound JK-31 (2,6-dihydroxybenzaldehyde 4-chlorobenzohydrazone) showed the best cytoprotective efficiency among the studied compounds including SIH. This compound significantly protected H9c2 cardiomyoblast cells against oxidative stress induced by various pro-oxidants, such as hydrogen peroxide, *tert*-butyl hydroperoxide, paraquat, epinephrine, *N*-acetyl-*p*-benzoquinone imine (a toxic metabolite of paracetamol) and 6-hydroxydopamine. The exceptional cytoprotective activity of JK-31 was confirmed using epifluorescence microscopy, where JK-31-treated H9c2 cells maintained a higher mitochondrial inner membrane potential in

the presence of a lethal dose of hydrogen peroxide than was observed with cells treated with SIH. Hence, this study demonstrates the deleterious role of free iron ions in oxidative injury and the potential of 2,6-dihydroxybenzaldehyde aroylhydrazones in the prevention of various types of cardiac injuries, highlighting the need for further investigations into these compounds.

## Keywords

Salicylaldehyde isonicotinoyl hydrazone; SIH; iron chelation; chelator; oxidative stress; 2,6-dihydroxybenzaldehyde.

## Introduction

Iron (Fe) is an indispensable micronutrient for all mammalian cells as well as the most abundant transition metal in the human body. It catalyzes biochemical reactions of vital importance for numerous essential cellular processes, such as respiration; syntheses of nucleic acids; proliferation and differentiation of cells; as well as regulation of gene expression.[1] An imbalance in Fe homeostasis may induce numerous disorders. Iron deficiency causes anemia, while Fe overload results in toxicity because of Fe-mediated oxidative stress. Free Fe ions readily cycle between their ferric ($Fe^{3+}$) and ferrous ($Fe^{2+}$) oxidation states and thus catalyze the Haber-Weiss reaction of superoxide radicals and hydrogen peroxide ($H_2O_2$) to generate hydroxyl radicals - the most reactive and toxic reactive oxygen species (ROS). Additionally, Fe-mediated toxicity may be present even without systemic Fe overload[2-4] and it has been associated with various cardiovascular diseases

such as ischemia/reoxygenation injury, cardiac dysrhythmias, myocarditis, heart failure, or cardiotoxicity of diverse redox-cycling agents.[5]

In addition to conventional therapies for the prevention and/or treatment of cardiovascular diseases, the use of various antioxidants has been proposed, but negative outcomes have generally been found.[6, 7] Unfortunately, most of the studies assessed various scavengers of already formed ROS rather than the actual prevention of ROS formation. This may be accomplished with Fe chelators forming complexes with Fe with no redox activity and thus inhibiting the formation of hydroxyl radicals.[8, 9]

Chelators are now well established in clinical practice to treat systemic Fe overload, where the key objective is the prevention of cardiac complications caused by long-term Fe deposition.[9-11] The potential of clinically used Fe chelators (desferrioxamine (DFO), deferiprone (L1) and deferasirox (ICL670A), Fig. 1) has also been examined in various oxidative stress-related pathologies without systemic Fe overload, such as in neurodegenerative diseases,[12-14] skin phototoxicity of UV irradiation,[15] cancer,[16, 17] and AIDS.[18] Another potential application of Fe chelation is the general prevention of cardiac ischemia/reperfusion injury[19] and cardiomyocyte oxidative injury, and in these cases, lipophilic Fe chelators with low molecular weight, including clinically used L1 and ICL670A as well as experimental compounds, showed promising cardioprotective potentials.[20-22]

Salicylaldehyde isonicotinoyl hydrazone (SIH) is a tridentate Fe chelator that can readily penetrate cellular membranes and tightly bind labile Fe ions.[23] Previous studies have clearly demonstrated its potential to protect the heart. SIH protected isolated primary cardiomyocytes and H9c2 cardiomyoblast cells from $H_2O_2$-induced oxidative injury[20, 23, 24] as well as against the toxicity caused by catecholamines[25] and *tert*-butyl hydroperoxide (*t*-BHP).[26] It displayed the best ratio of cytoprotective activity against cellular oxidative injury to its own toxicity among various chelators,

including the above-mentioned DFO, L1 and ICL-670A.[26] SIH also afforded protection against the cardiotoxicity of anthracycline daunorubicin (DAU) *in vitro* as well as *in vivo* using isolated rat cardiomyocytes [21] and a model of anthracycline-induced heart failure in rabbits,[27, 28] respectively. However, the main limitation of SIH is its fast degradation in biological environments along with its relatively short biological half-life.[29, 30]

The aim of this study was to design and synthesize novel SIH analogues with increased cytoprotective properties. The free rotation of the bond between the hydrazone and phenol fragments can slightly decrease the chelation ability of SIH due to the formation of ineffective conformers. Thus, we replaced the salicylaldehyde moiety with a symmetrical 2,6-dihydroxybenzaldehyde group, which minimizes the abovementioned influence of the bond rotation, and we prepared a series of novel 2,6-dihydroxybenzaldehyde aroylhydrazones (Fig. 2). Furthermore, the additional hydroxyl group in position 6 adjacent to the hydrazone can also affect its stability towards hydrolysis. To characterize these novel derivatives, we examined their (***1***) Fe chelating activity in solution and in H9c2 rat embryonic cardiomyoblast cells; (***2***) cytoprotective potential against $H_2O_2$-induced toxicity to H9c2 cells; (***3***) inherent toxicity (non-cancerous H9c2 cells) and anticancer activity using MCF-7 breast adenocarcinoma and HeLa cervical carcinoma cells; (***4***) redox properties; and (***5***) stability against hydrolysis in a cell culture medium.

## Experimental procedures

**General.** The prepared compounds were characterized by their melting points, $^1$H NMR and $^{13}$C NMR spectra. The purities of all reported compounds were determined by elemental analysis. The chemicals were obtained from following suppliers: Penta (Czech Republic) or Merck (Germany). All were of the highest available purity. Merck aluminum plates with silica gel 60 $F_{254}$ and Merck Kieselgel 60 (0.040-0.063 mm) were used for thin layer chromatography and column

chromatography, respectively. Melting points were determined with a Büchi B-545 (BUCHI Labortechnik AG, Flawil, Switzerland) and are uncorrected. $^{1}H$ and $^{13}C$ NMR spectra were measured on a VNMR S500 NMR spectrometer (Varian, Palo Alto, CA, USA). The elemental analyses were carried out on an Automatic Microanalyzer EA1110CE (Fisons Instruments S.p.A., Milano, Italy). The chelator SIH was prepared as described previously.[31]

*2,6-Dimethoxybenzaldehyde* (**11**):[32] To a solution of 1,3-dimethoxybenzene (**10**, 5.54 g, 40.1 mmol) in THF (15 mL) was added a solution of n-BuLi in hexane (30 mL, 1.6 mol/L, 48.0 mmol) at 0 °C over 20 min. The reaction mixture was stirred at rt for 30 min, again cooled to 0 °C and DMF (3.7 mL, 48 mmol) was added dropwise. The reaction mixture was stirred for 1 h at rt, and then the mixture was concentrated to approximately half its volume under reduced pressure. Then, 10% aqueous HCl (50 mL) was added at 0 °C, and the reaction mixture was stirred for 12 h. The resulting mixture was extracted with EtOAc (3 × 50 mL), and the combined organic phases were washed with brine, dried over $Na_2SO_4$ and evaporated. The product (**11**) was purified using column chromatography (mobile phase: hexane/ethyl acetate, 4:1 – 2:1) and recrystallized from aq. EtOH. Yield: 88% (5.9 g) as a yellowish solid. Mp 96-97 °C (lit.[33] 95.5-97 °C). $^{1}H$ NMR (500 MHz, $CDCl_3$) δ 10.50 (s, 1H), 7.44 (t, $J$ = 8.5 Hz, 1H), 6.57 (d, $J$ = 8.5 Hz, 2H), 3.88 (s, 6H). $^{13}C$ NMR (126 MHz, $CDCl_3$) δ 189.32, 162.10, 135.84, 114.25, 103.79, 55.97.

*2,6-Dihydroxybenzaldehyde* **(DHBA):**[34] $AlCl_3$ (1.30 g, 9.76 mmol) was mixed with $CH_2Cl_2$ (15 mL) at 0 °C. To this suspension, a solution of 2,6-dimethoxybenzaldehyde (**11**, 0.5 g, 3.0 mmol) in $CH_2Cl_2$ (10 mL) was added dropwise at rt, and the mixture was stirred at rt for 24 h. Then, 10% aqueous HCl (25 mL) was carefully added to the mixture under vigorous stirring. After 10 min, the aqueous phase was separated and extracted with EtOAc (3 × 25 mL). The combined organic phases were dried over $Na_2SO_4$ and evaporated. The product (**DHBA**) was purified using column

chromatography (mobile phase: hexane/ethyl acetate, 7:1). Yield: 63% (0.26 g) as a yellowish solid. Mp 154-156 °C (lit.[34] 156-157 °C). $^{1}$H NMR (500 MHz, DMSO) δ 11.25 (s, 2H), 10.25 (s, 1H), 7.35 (t, *J* = 8.3 Hz, 1H), 6.36 (d, *J* = 8.3 Hz, 2H). $^{13}$C NMR (126 MHz, DMSO) δ 194.50, 162.23, 139.11, 110.18, 106.83.

**General procedure for the preparation of 2,6-dihydroxybenzaldehyde hydrazones 1-9.** 2,6-Dihydroxybenzaldehyde (**DHBA**, 0.07 g, 0.5 mmol) and the appropriate hydrazide (0.75 mmol) were dissolved in ethanol (96%, 5 mL) and five drops of conc. acetic acid were added. The reaction mixture was refluxed for 2-24 h and then cooled to 5 °C and kept at this temperature as long as crystallization was observed (1-5 days). In some cases (products **3** and **9**), the solution was diluted with water to initiate crystallization. Finally, the product was isolated by filtration, washed with cold ethanol and then dried.

*2,6-Dihydroxybenzaldehyde isonicotinoyl hydrazone* (**1**): Commercially available isoniazide was used. The reaction mixture was refluxed for 24 h. Yield: 97 % as a white solid. Mp 283-285 °C. $^{1}$H NMR (500 MHz, DMSO) δ 12.33 (s, 1H), 11.08 (s, 2H), 8.97 (s, 1H), 8.80 (d, *J* = 5.3 Hz, 2H), 7.87 – 7.83 (m, 2H), 7.12 (t, *J* = 8.2 Hz, 1H), 6.38 (d, *J* = 8.2 Hz, 2H). $^{13}$C NMR (126 MHz, DMSO) δ 161.12, 158.70, 150.58, 147.77, 139.87, 132.90, 121.62, 106.74, 106.22. Anal. Calcd. for $C_{13}H_{11}N_3O_3$: C, 60.70; H, 4.31; N, 16.33; Found: C, 60.39; H, 4.33; N, 16.28.

*2,6-Dihydroxybenzaldehyde nicotinoyl hydrazone* (**2**): Commercially available nicotinoyl hydrazide was used. The reaction mixture was refluxed for 6 h. Yield: 81% as a white solid. Mp 271-272 °C. $^{1}$H NMR (500 MHz, DMSO-$d_6$) δ 12.28 (s, 1H), 11.09 (s, 2H), 9.11 (d, *J* = 2.3 Hz, 1H), 8.95 (s, 1H), 8.78 (dd, *J* = 4.9, 1.7 Hz, 1H), 8.30 (dt, *J* = 8.1, 2.0 Hz, 1H), 7.60 (dd, *J* = 7.9, 4.9 Hz, 1H), 7.11 (t, *J* = 8.2 Hz, 1H), 6.38 (d, *J* = 8.2 Hz, 2H). $^{13}$C NMR (126 MHz, DMSO) δ

161.24, 158.64, 152.65, 148.79, 147.18, 135.57, 132.73, 128.62, 123.83, 106.73, 106.27. Anal. Calcd. for $C_{13}H_{11}N_3O_3$: C, 60.70; H, 4.31; N, 16.33; Found: C, 60.31; H, 4.52; N, 15.92.

*2,6-Dihydroxybenzaldehyde benzohydrazone monohydrate* (**3**): The benzohydrazide used in this reaction was prepared according to a published procedure.[35] The reaction mixture was refluxed for 24 h. The final solution was diluted with water to initiate the crystallization. Yield: 57% as a white solid. Mp 249-251 °C. $^1$H NMR (500 MHz, DMSO) δ 12.10 (s, 1H), 11.12 (s, 2H), 8.95 (s, 1H), 7.99 – 7.88 (m, 2H), 7.63 – 7.58 (m, 1H), 7.57 – 7.51 (m, 2H), 7.10 (t, $J$ = 8.2 Hz, 1H), 6.38 (d, $J$ = 8.2 Hz, 2H). $^{13}$C NMR (126 MHz, DMSO) δ 162.65, 158.57, 146.58, 132.79, 132.48, 132.16, 128.73, 127.77, 106.69, 106.40. Anal. Calcd. for $C_{14}H_{12}N_2O_3.H_2O$: C, 61.31; H, 5.15; N, 10.21; Found: C, 61.35; H, 5.18; N, 10.13.

*2,6-Dihydroxybenzaldehyde 4-methylbenzohydrazone monohydrate* (**4**): The 4-methylbenzohydrazide used in this reaction was prepared according to a published procedure.[35] The reaction mixture was refluxed for 2 h. Yield: 92% as a white solid. Mp 255-257 °C. $^1$H NMR (500 MHz, DMSO) δ 12.04 (s, 1H), 11.12 (s, 2H), 8.94 (s, 1H), 7.86 (d, $J$ = 8.0 Hz, 2H), 7.34 (d, $J$ = 8.0 Hz, 2H), 7.09 (t, $J$ = 8.2 Hz, 1H), 6.37 (d, $J$ = 8.2 Hz, 2H), 2.38 (s, 3H). $^{13}$C NMR (126 MHz, DMSO) δ 162.50, 158.55, 146.29, 142.28, 132.41, 129.92, 129.28, 127.80, 106.69, 106.45, 21.23. Anal. Calcd. for $C_{15}H_{14}N_2O_3.H_2O$: C, 62.49; H, 5.59; N, 9.72; Found: C, 62.37; H, 5.65; N, 9.68.

*2,6-Dihydroxybenzaldehyde 4-chlorobenzohydrazone monohydrate* (**5**, JK-31): The 4-chlorobenzohydrazide used in this reaction was prepared according to a published procedure.[35] The reaction mixture was refluxed and stirred for 24 h. Yield: 53% as a white solid. Mp 276-278 °C. $^1$H NMR (500 MHz, DMSO) δ 12.18 (s, 1H), 11.11 (s, 2H), 8.94 (s, 1H), 7.97 (d, $J$ = 8.6 Hz, 2H), 7.62 (d, $J$ = 8.6 Hz, 2H), 7.10 (t, $J$ = 8.2 Hz, 1H), 6.37 (d, $J$ = 8.2 Hz, 2H). $^{13}$C NMR (126 MHz,

DMSO) δ 161.62, 158.63, 146.91, 137.06, 132.65, 131.53, 129.73, 128.89, 106.73, 106.36. Anal. Calcd. for $C_{14}H_{11}ClN_2O_3.H_2O$: C, 54.47; H, 4.24; N, 9.07; Found: C, 54.20; H, 4.30; N, 8.93.

*2,6-Dihydroxybenzaldehyde 3-chlorobenzohydrazone monohydrate* (**6**): The 3-chlorobenzohydrazide used in this reaction was prepared according to a published procedure.[35] The reaction mixture was refluxed for 4 h. Yield: 76% as a white solid. Mp 226-228 °C. $^1$H NMR (500 MHz, DMSO) δ 12.18 (s, 1H), 11.09 (s, 2H), 8.95 (s, 1H), 8.00 (t, *J* = 1.9 Hz, 1H), 7.93 – 7.89 (m, 1H), 7.69 – 7.66 (m, 1H), 7.58 (t, *J* = 7.9 Hz, 1H), 7.10 (t, *J* = 8.2 Hz, 1H), 6.38 (d, *J* = 8.2 Hz, 2H). $^{13}$C NMR (126 MHz, DMSO) δ 161.23, 158.64, 147.15, 134.79, 133.56, 132.71, 131.99, 130.79, 127.49, 126.64, 106.73, 106.32. Anal. Calcd. for $C_{14}H_{11}ClN_2O_3.H_2O$: C, 54.47; H, 4.24; N, 9.07; Found: C, 54.11; H, 4.27; N, 9.11.

*2,6-Dihydroxybenzaldehyde 4-bromobenzohydrazone monohydrate* (**7**): The 4-bromobenzohydrazide used in this reaction was prepared according to a published procedure.[36] The mixture was refluxed for 2 h. Yield: 85% as a white solid. Mp 276-278 °C. $^1$H NMR (500 MHz, DMSO) δ 12.17 (s, 1H), 11.10 (s, 2H), 8.94 (s, 1H), 7.90 (d, *J* = 8.6 Hz, 2H), 7.76 (d, *J* = 8.6 Hz, 2H), 7.10 (t, *J* = 8.2 Hz, 1H), 6.37 (d, *J* = 8.2 Hz, 2H). $^{13}$C NMR (126 MHz, DMSO) δ 161.71, 158.60, 146.91, 132.62, 131.87, 131.80, 129.86, 126.00, 106.70, 106.34. Anal. Calcd. for $C_{14}H_{11}BrN_2O_3.H_2O$: C, 47.61; H, 3.71; N, 7.93; Found: C, 47.75; H, 3.73; N, 7.84.

*2,6-Dihydroxybenzaldehyde pyrazine-2-carbohydrazone* (**8**): The pyrazine-2-carbohydrazide used in this reaction was prepared according to a published procedure.[37] The mixture was refluxed and stirred for 4 h. Yield: 72% as a white solid. Mp 320 °C (with decomposition). $^1$H NMR (500 MHz, DMSO) δ 12.70 (s, 1H), 11.12 (s, 2H), 9.26 (d, *J* = 1.5 Hz, 1H), 9.14 (s, 1H), 8.92 (d, *J* = 2.5 Hz, 1H), 8.79 (dd, *J* = 2.5, 1.5 Hz, 1H), 7.11 (t, *J* = 8.2 Hz, 1H), 6.37 (d, *J* = 8.2 Hz, 2H). $^{13}$C NMR (126 MHz, DMSO) δ 159.52, 158.80, 148.65, 148.10, 144.43, 144.35, 143.59, 132.82,

106.72, 106.45. Anal. Calcd. for $C_{12}H_{10}N_4O_3$: C, 55.81; H, 3.90; N, 21.70; Found: C, 55.46; H, 3.85; N, 21.34.

2*,6-Dihydroxybenzaldehyde cyclohexanecarbohydrazone* (**9**): The cyclohexanecarbohydrazide used in this reaction was prepared according to a published procedure.[35] The reaction mixture was refluxed for 7 h. The final solution was diluted with water to initiate the crystallization. Yield: 77 % as a white solid. Mp 226-230 °C. $^1$H NMR (500 MHz, DMSO) δ 11.53 (s, 1H), 11.00 (s, 2H), 8.64 (s, 1H), 7.05 (t, $J$ = 8.2 Hz, 1H), 6.33 (d, $J$ = 8.2 Hz, 2H), 2.24 – 2.14 (m, 1H), 1.80 – 1.70 (m, 4H), 1.67 – 1.59 (m, 1H), 1.46 – 1.34 (m, 2H), 1.31 – 1.12 (m, 3H). $^{13}$C NMR (126 MHz, DMSO) δ 171.25, 158.36, 144.73, 132.19, 106.63, 106.29, 42.80, 29.11, 25.53, 25.34. Anal. Calcd. for $C_{14}H_{18}N_2O_3$: C, 64.11; H, 6.92; N, 10.68; Found: C, 63.75; H, 6.93; N, 10.49.

**Cell culture.** The H9c2 cardiomyoblast cell line[38] was obtained from the American Type Culture Collection (ATCC, USA). Cells were cultured as described previously.[39, 40] Twenty-four hours before the experiments, the medium was replaced with serum- and pyruvate-free DMEM (Sigma, Germany). Serum deprivation was used to stop cellular proliferation to mimic the situation in post-mitotic cardiomyocytes. However, to maintain the same protein content, the medium was supplemented with the corresponding amount of BSA (4.7 mg/mL). Pyruvate-free medium was used because pyruvate is an antioxidant and may interfere with ROS-induced toxicity.

The MCF-7 human breast adenocarcinoma cell line (ECACC; Salisbury, UK) and the human cervical carcinoma (HeLa) cell line (ATCC; Manassas, VA, USA) were cultured as described previously.[41]

DMSO was used to dissolve the lipophilic compounds. The final concentration of DMSO was 0.2 % in all experimental groups, which had no effect on cellular viability.

**Calcein assay for measuring chelating activity of studied compounds in HBS buffer.**[42] Determinations of the calcein fluorescence intensity were used to evaluate the Fe chelation efficiencies of the studied compounds as described previously by our group.[39] Solution of Fe-chelator under investigation was added to give a final concentration of 100 μM. The change in fluorescence intensity was measured at 25 °C for 10 min using a Tecan plate reader. The Fe-chelation activity of a given compounds is expressed as a percentage of the efficiency of SIH (100 %).

**Calcein-AM assay for determining the cell membrane permeability of studied compounds and their access to the intracellular labile Fe pool.** The experiments were performed according to Glickstein *et al.*[43] with some modifications as described previously by our group.[39, 40] The intracellular fluorescence was monitored as a function of time (1 min before and 10 min after the addition of the studied compounds at a concentration of 100 μM; $\lambda_{ex}$ = 488 nm; $\lambda_{em}$ = 530 nm) using a Tecan Infinite 200 M micro-plate spectrophotometer (Tecan, Austria).

**Neutral red uptake assay for the assessment of cellular viability.** The cellular viabilities of H9c2, MCF-7 and HeLa cells were determined using a neutral red assay as described previously by our group.[39, 40] H9c2 cells (10,000 cells per well) were incubated with the studied compounds and $H_2O_2$ or other pro-oxidants for 24 h to measure their cytoprotective effects. The toxicities (H9c2 cells) and antiproliferative effects (MCF-7 and HeLa cells) of the tested compounds were measured after 72 h of incubation. The viability of each group was expressed as a percentage relative to the untreated control (100 %).

**Ascorbate oxidation assay for the analysis of the redox activity of the Fe-chelator complexes.** The ability of the Fe complexes of the novel SIH analogues to mediate the oxidation of ascorbate was examined using an established protocol[44, 45] with step-by-step procedure described

in our previous study.[41] The solutions were assayed at Fe-binding equivalents (IBE) of 0.1 (excess Fe), 1 (complexes of Fe with the studied compounds) and 3 (excess of the studied compounds). The redox activities of Fe chelators EDTA and DFO have been well characterized,[46] and therefore they were used as the positive and negative controls, respectively. The decrease in absorbance between the two time points ($T_{10} - T_{40}$) was calculated and is expressed as the decrease in absorbance.

**Stability study.** A Nexera X2 UHPLC instrument with a photodiode array detector (Shimadzu, Japan) was emplyed to assay concentrations of the SIH analogues. The data were processed using LabSolutions software (v. 5.55, 2013, Shimadzu, Japan). An Ascentis C18 column (100 x 3 mm, 3 μm) with the corresponding guard column (both Supelco, PA, USA) were used as a stationary phase. The column oven was set at 25 °C. The mobile phase consisted of a component A (an aqueous solution of 5 mM $NaH_2PO_4$ and 1 mM EDTA; without pH correction) and a component B (methanol). Their ratios (v/v) as well as detection wavelengths used for the assay were optimized for each compound individually (Table S2). A flow rate of mobile phase was 0.3 mL/min. Ten μL of the samples were injected onto the column. The selectivity was tested by comparing the chromatograms obtained from analysis of the blanks with that monitored for the spiked samples. The linearity, precision and accuracy of the assay were evaluated for both media (with and without BSA) according to the FDA guidelines on Bioanalytical Method Validation[47] over the range of 10 – 100 μM and fit the criteria well.

An appropriate volume of the standard solution of each compound (100 mM in DMSO) was added to preheated aliquots (n = 3) of the cell culture medium with or without BSA. The final concentration of the compound in the media was 100 μM. These samples were incubated at 37 °C for 24 h. At selected times (0, 0.5, 1, 3, 6 and 24 h), 100 μL aliquots of the medium without BSA

were diluted with methanol (1:1) and injected onto the column, whereas 100 µL aliquots of the medium with BSA were transferred to Eppendorf tubes, and BSA proteins were precipitated with 300 µL of ice-cold methanol. Centrifugation (10,000 rpm, 10 min, 4 °C) was used to divide proteins from the supernatant which was analyzed.

**Determination of the mitochondrial inner membrane potential.** Photomicrographs were obtained as described previously by our group.[39] The red and green fluorescence was quantitated using a Tecan Infinite 200 M plate reader (Tecan, Austria).

**Measurements of the inner tryptophan fluorescence.** The ability of SIH and JK-31 to bind to BSA was determined by measuring of quenching of the inner tryptophan fluorescence.[48, 49] BSA was dissolved in buffer (120 mM NaCl, 10 mM KCl, and 30 mM TRIS at pH = 7.4) to a final concentration of 0.6 µM. The fluorescence ($\lambda_{ex}$ = 280 nm; $\lambda_{em}$ = 350 nm) was measured 1 min before and 10 min after the addition of warfarin (used as a positive control) and SIH and JK-31 at concentrations of 10, 30, 100 and 300 µM using a spectrophotometer Tecan Infinite 200 M (Tecan, Austria).

**Data analysis.** SigmaStat for Windows 3.5 (SPSS, USA) was used for statistical analysis. The data are presented as the mean ± standard deviation (SD). Statistical significance was assessed using ANOVA with a Bonferroni post hoc test. Half-maximal toxic concentration ($TC_{50}$), half-maximal inhibitory concentration ($IC_{50}$) and half-maximal effective concentration ($EC_{50}$) were calculated using CalcuSyn 2.0 software (Biosoft, UK). The graphs were prepared using GraphPad Prism 7 for Windows (GraphPad Software, USA).

# Results and Discussion

**Chemistry.** 2,6-Dihydroxybenzaldehyde (DHBA) was prepared according to previously published procedures with some modifications. In the first step, 1,3-dimethoxybenzene (**10**) was lithiated with BuLi and subsequently formylated using *N*,*N*-dimethylformamide (DMF).[32] Cleavage of the resulting 2,6-dimethoxybenzaldehyde (**11**) under mild reaction conditions using excess aluminum chloride at room temperature gave DHBA in moderate yield (Scheme 1).[34]

The 2,6-dihydroxybenzaldehyde aroylhydrazones **1**-**8** and alkanoylhydrazone **9** were prepared *via* the condensation of DHBA with the corresponding hydrazides in boiling ethanol (Scheme 2). Upon cooling the reaction mixtures, pure products **1, 2** and **4**-**8** crystallized from the reaction mixtures in sufficient purity. In the case of hydrazones **3** and **9**, a small amount of water was added to the cold reaction mixture to initiate the crystallization.

**Determination of Fe-chelating efficiency in solution.** Chelation efficiencies of the studied compounds were firstly examined in a cell-free system. The increase in fluorescence (induced by the displacement of Fe ions from the calcein complex ) was monitored for 10 min after the addition of the studied compounds (all 100 μM). As apparent from Fig. 3, all of the studied compounds (**1**-**9**) displayed strong chelating activities, with the exception of starting substance DHBA. Compounds **1**, **3** and **8** showed rapid chelation, while the effects of compounds **4**, **5**, **6** and **7**, with substituted benzoyl groups, had slower onsets (Fig. 3A); however, all of these compounds displayed better chelating activity than parent chelator SIH at t = 10 min (Fig. 3B). Isonicotinoyl derivative **1** and 4-chlorobenzoyl derivative **5** (JK-31) exhibited the highest efficacies. The only alkanoyl derivative, 2,6-dihydroxybenzaldehyde cyclohexanecarbohydrazone (**9**), showed a significantly lower chelating efficiency than SIH.

**Determination of cell membrane permeability and access to the intracellular labile Fe.** The abilities of the studied compounds to access the labile Fe pool inside the H9c2 cells were

compared using the calcein-AM assay. Increases in the intracellular fluorescence were measured during the 10-min incubation of the cells with the studied compounds (all 100 μM concentration). The results are shown as the percentages of the chelating effectiveness relative to reference chelator SIH at t = 10 min (Fig. 4). In previous studies, SIH was more effective and faster at dequenching intracellular calcein than clinically used Fe chelators L1 and ICL670A.[26, 39] All of the newly prepared compounds showed chelating activities comparable to SIH except for compound **4**, which displayed a chelating efficiency that was slightly but significant lower (18%) than that of SIH. DHBA showed a low, but significant chelating activity compared to control (11 % of the chelating activity of SIH).

**Inherent toxicity of the studied compounds.** The own toxicities of each compound toward H9c2 cells were examined using the neutral red uptake assay. To compare the individual agents, their $TC_{50}$ values (the concentrations causing 50 % viability loss compared to untreated control cells) were determined. After 24 h, the toxicities of the studied a were very low ($TC_{50}$ > 300 μM; data not shown), therefore we incubated the cells with the studied compounds for 72 h. (Table 1). All of the studied agents induced dose-dependent decreases in cellular viability (Fig. 5). Compound **6** was the only compound that exhibited significantly higher toxicity than chelator SIH; $TC_{50}$ (**6**) = 6.5 μM and $TC_{50}$ (SIH) = 15.3 μM. Hydrazones **8** and **9** and starting substance DHBA caused lower reductions in cell viability. Nonetheless, the majority of the studied hydrazones (**1**-**5**, **6**, **7**) displayed inherent toxicities similar to that of parent chelator SIH.

**Cytoprotective potential of the studied compounds against the oxidative stress.** The ability of the studied compounds SIH, DHBA and hydrazones **1**-**9** to protect H9c2 cells against oxidative stress induced by 200 μM $H_2O_2$ was evaluated by the neutral red uptake assay after 24 h (Fig. 6). The $EC_{50}$ values, *i.e.,* concentrations reducing the $H_2O_2$ toxicity to half of the viability of untreated

control cells, and their cytoprotective effectiveness at concentrations of 30 μM and 100 μM are summarized in Table 1.

SIH and hydrazones **6-8** protected cells against the toxicity caused by $H_2O_2$ in similar dose-dependent manner. They protected H9c2 cells significantly at a concentration of 30 μM. However, even in the highest achievable concentration (600 μM), they were not able to increase cellular viability above half of the untreated control cells, and therefore we could not calculate the $EC_{50}$ values. Compounds **1-5** exhibited better protective properties than SIH. Similarly, they significantly protected cells at a concentration of 30 μM, but they were more efficient. Compound **5** (JK-31) significantly protected cells at a concentration of 10 μM and showed the lowest $EC_{50}$ value. Therefore, the protective properties of this compound were studied in more detail, and its effectiveness was compared with that of SIH (see below). Alkanoyl derivative **9** and DHBA displayed lower protective effects than SIH.

In this study, we corroborated the previously reported ability of SIH to protect H9c2 cells from model oxidative stress.[39, 40] However, here we used DMEM supplemented with bovine serum albumin (BSA) to maintain the same protein content as in the medium with fetal bovine serum (FBS). In previous studies, DMEM was employed without serum or albumin, which could cause some discrepancies between the previous results and those presented herein. Therefore, we determined the stability and cytoprotective effects in DMEM without BSA as well and found that SIH and halobenzoyl hydrazones **5**, **6** and **7** displayed better cytoprotective effect in DMEM without BSA supplementation (Fig. S1; Table S1). These results are in agreement with the increased stability of compounds **5**, **6** and **7** in DMEM without BSA (Fig. S2). As SIH exhibited similar stabilities in both media, we assume that its protein binding caused the decrease of its

cytoprotective effect in BSA-containing medium. This hypothesis is supported by the ability of SIH to quench tryptophan fluorescence in BSA (Fig. S3).

**Evaluation of the redox activity of Fe complexes of the studied compounds to catalyze the oxidation of ascorbate.** The ascorbate oxidation assay was used to assess the Fe complexes of the chelators with respect to affect the oxidation of a physiological substrate, ascorbate. The chelator DFO was used as a negative (antioxidant) control, whereas EDTA was used as a positive (pro-oxidant) control. As previously described, the Fe-DFO complex exhibited a typical antioxidant effect,[50] whereas the Fe-EDTA complex promoted higher ascorbate oxidation (Fig. 7). The Fe-SIH complex as well as the Fe complexes with compounds **1**, **2**, **3**, **5**, **6**, **7** and **8** displayed antioxidant activities similar to that of the Fe complex with DFO. Compounds **4** and **9** significantly reduced ascorbate oxidation only at an IBE of 3, and DHBA did not significantly influence ascorbate oxidation. None of the studied compounds, except EDTA, exhibited redox cycling at any IBE expressed as an increase in ascorbate oxidation (Fig. 7).

**Stability of the studied compounds in cell culture medium.** The stabilities of novel SIH analogues **1**-**9** were assessed using HPLC analysis following 24 h of incubation of the compounds in DMEM supplemented with BSA without cells (Fig. 8). The initial concentration of the studied compounds was 100 μM, which reflected the maximal plasmatic concentration (108 μM) determined in the pilot *in vivo* pharmacokinetics study with SIH in rabbits.[30] For clarity, we divided the studied compounds into three groups according to their structure. The first group included SIH and its closest derivatives, **1** and **2**, which each bear an (iso)nicotinoyl group (Fig. 8A). All these compounds showed similar rapid degradation profiles. After only 3 h, approximately 50 % of these compounds had decomposed, and by the end of the experiment, near complete decomposition of these compounds was observed. Thus, unexpectedly, the additional hydroxyl group in the 6-

position of the 2,6-dihydroxybenzaldehyde moiety did not influence the stability of the adjacent hydrazone bond. The second group consists of unsubstituted and monosubstituted benzohydrazones (compounds **3**-**7**; Fig. 8B). These derivatives displayed higher stabilities than SIH. The concentrations of these compounds had been reduced to approximately half of the initial concentration after 12-16 h of incubation, and by the end of the experiment, approximately 25 % of the compounds remained. Similar stability profiles were also exhibited by compound **8** and **9** (Fig. 8C), and their concentrations decreased by approximately 50% after 12-16 h of incubation. The greater stability of derivatives **3**-**7** and **9** can be attributed to their higher lipophilicity when compared to those of SIH or derivatives **1** and **2** (Table 1).

**Comparison of the cytoprotective properties of SIH and compound 5 (JK-31).** The JC-1 probe was employed to determine the mitochondrial inner membrane potentials ($\Delta\Psi_m$ values), and it was observed by epifluorescence microscopy (Fig. 9) and quantified spectrofluorometrically (Fig. 10). H9c2 cells were incubated in DMEM with BSA for 24 h with 100 μM SIH or the most active analogue (JK-31) alone or in combination with $H_2O_2$ (200 μM). SIH and JK-31 induced slight but significant reductions in the red fluorescence intensity and slight increases in green fluorescence, indicating slow and transient losses of $\Delta\Psi_m$. SIH showed a decrease of approximately 20 % relative to the control group, while JK-31 showed a decrease of only 10 %. The $H_2O_2$-treated cells displayed a conspicuous transition to green fluorescence, indicating complete $\Delta\Psi_m$ dissipation, whereas SIH and JK-31 significantly protected the H9c2 cells from the $H_2O_2$-induced $\Delta\Psi_m$ loss with JK-31 providing significantly greater protection than SIH.

The cytoprotective efficiencies of SIH and JK-31 were also evaluated on H9c2 cells against the toxicity of other pro-oxidants that are used as the basic models of oxidative damage in various pathological conditions (Fig. 11). We observed that SIH and particularly JK-31 significantly

protected H9c2 cells against the viability reduction induced by all the tested pro-oxidant xenobiotics in a dose-dependent manner. The excellent cytoprotective efficacy of JK-31 was observed in the experiments in which the H9c2 cells were exposed to *tert*-butyl hydroperoxide (*t*-BHP), a model oxidative stressor that is more stable than $H_2O_2$ (Fig. 11B), and *N*-acetyl-*p*-benzoquinone imine (NAPQI), a toxic metabolite of the analgesic paracetamol (Fig. 11C). NAPQI is an ROS that causes oxidative injury by binding cellular macromolecules, which leads to subsequent cell death.[51] JK-31 significantly protected H9c2 cells at concentrations as low as 10 μM, while SIH showed protective effects starting at 10 μM (NAPQI) or 100 μM (*t*-BHP). In these experiments, JK-31 always displayed significantly higher protective efficiencies than SIH at 10, 30 and 100 μM concentrations.

Two catecholamines, epinephrine (EPI; 100 μM; Fig. 11D) and 6-hydroxydopamine (6OHDA; 100 μM; Fig. 11E), were also used in this study because there is an increasing evidence that the catecholamine-induced cardiac injury involves the Fe-mediated ROS formation.[52] Previous studies have shown the promising cytoprotective properties of SIH against oxidative damage induced by the catecholamines EPI and isoprenaline to H9c2 cells.[25] Compared with another study conducted under the same conditions but with Fe chelators used in clinical practice (DFO, L1 and ICL670A), SIH achieved better protective efficacy than the clinically used Fe chelators.[22] In this study, JK-31 also significantly reduced the cytotoxicity caused by both of the studied catecholamines and displayed a higher effectiveness than SIH at all concentrations with significant cytoprotective effects. As catecholamines undergo spontaneous oxidation resulting in the formation of reactive redox cycling intermediates, [53] we assessed the protective effect of SIH and JK-31 against oxidative damage caused by EPI and 6OHDA that had been preoxidized for 24 h (oxEPI; Fig. 11F, and ox6OHDA; Fig. 11G, respectively). JK-31 significantly protected H9c2 cells starting at

concentrations of 10 μM and always displayed significantly higher protective potentials than SIH except at 300 μM in the experiment with ox6OHDA.

We also investigated the protective effects of JK-31 against the cytotoxicity induced by the redox cycling herbicide paraquat (Fig. 11H)[54] and anthracycline anticancer agent daunorubicin (DAU; Fig. 11I). Anthracyclines induce ROS formation through several pathways, including one-electron reduction leading to the formation of a semiquinone free radical. They may also increase the redox-active Fe pool by generating superoxide radicals, which can induce the Fe release from ferritin.[55] SIH significantly reduced their toxicities starting at a concentration of 100 μM, while JK-31 was effective from 10 μM (paraquat) or 30 μM (DAU). JK-31 provided greater protection than SIH at all tested concentrations, but a statistically significant difference was only observed at 30 and 100 μM concentrations of paraquat.

**Antiproliferative effects.** Fe chelators have shown potential in anticancer therapies.[9] Cancer cells have a high Fe demand due to their quick replication rate.[56] Limiting the Fe available to cancer cells may therefore block their proliferation. The antiproliferative effects of SIH and its analogues **1**-**9** were studied on MCF-7 breast adenocarcinoma cells (Fig. 12) after 72 h of incubation. Previous studies have shown that chelator SIH demonstrated moderate cytotoxic activity compared to some other anticancer drugs.[57, 58] In this study, SIH was used as a control for the newly prepared analogues. Only compounds **5** (JK-31) and **7** showed higher antiproliferative activities than SIH. The remaining compounds (**1**-**4**, **6**, **8**, and **9**) had similar or lower antiproliferative activities than SIH. As expected, DHBA displayed the lowest activity (Table 2).

Similar results were also obtained with HeLa cervical carcinoma cells (Fig. 12). DHBA and compound **8** exhibited poor antiproliferative activities. On the other hand, compounds **5**, **7** and **4**

showed better antiproliferative activities than SIH. Other compounds displayed effects similar to that of SIH (Table 2).

# Conclusions

In clinical practice, chelators of Fe represent a well-established therapy of diseases with chronic Fe overload, especially the β-thalassemia.[59] Chelation therapy is now being specifically evaluated and optimized for myocardial Fe removal and/or prevention of myocardial Fe accumulation.[60] Fe chelators have also been studied in cardiovascular diseases without systemic Fe overload to reduce Fe-mediated intramyocardial oxidative stress. Earlier studies suggested that the experimental Fe chelator SIH had the most promising properties in this field. However, the free rotation of the bond between the hydrazone and phenol fragments in SIH can hinder its chelation ability due to the formation of ineffective conformers. Therefore, we designed and prepared a series of 2,6-dihydroxybenzaldehyde-type analogues of SIH and assessed their structure-activity relationships. We found that all of the prepared compounds (**1**-**9**) showed excellent chelating properties comparable to that of the parent SIH. Regarding their cytoprotective activities in H9c2 cardiomyoblast cells, only alkanoylhydrazone **9** showed a significantly reduced ability to protect H9c2 cardiomyoblasts from model $H_2O_2$-induced toxicity. All other aroylhydrazones (**1**-**8**) showed comparable or better cytoprotective activities than the parent SIH. Thus, an aromatic R substituent greatly enhances the cytoprotective properties. It should be noted that 2,6-dihydroxybenzaldehyde, the common metabolite of compounds **1**-**9**, was not responsible for any of the biological activities of compounds **1**-**9** evaluated in this study. The R substituent also plays a major role in the hydrolytic stability of the studied hydrazones in aqueous media: (iso)nicotinoyl hydrazones **1** and **2** are significantly less stable than the more lipophilic aroylhydrazones **3**-**7**.

Among the studied compounds, analogue **5** (JK-31, 2,6-dihydroxybenzaldehyde 4-chlorobenzohydrazone) showed the most promising properties. JK-31 displayed a cytotoxicity and chelating activity similar to those of SIH, but it exhibited increased stability in cellular media and

better cytoprotective properties against oxidative damage of H9c2 cells induced by $H_2O_2$. JK-31 protected half of the H9c2 cells against the toxic effects of $H_2O_2$ at a concentration of 18.2 μM, whereas SIH was uncapable to protect 50 % of cells even at 600 μM. Moreover, JK-31 showed a significantly higher cytoprotective efficiency than SIH against various pro-oxidant xenobiotics, including *tert*-butyl hydroperoxide, the redox cycling herbicide paraquat, parent and preoxidized epinephrine and 6-hydroxydopamine, and the toxic metabolite of paracetamol *N*-acetyl-*p*-benzoquinone imine. Thus, JK-31 can serve as a new lead hydrazone-type antioxidant Fe chelating agent for further structural refinements and *in vitro* and *in vivo* studies.

## Acknowledgements

This study was supported by the project EFSA-CDN (No. CZ.02.1.01/0.0/0.0/16_019/0000841) co-funded by ERDF, Czech Science Foundation (project 13-15008S) and the Charles University (project SVV 260 416).

## Abbreviations

6OHDA, 6-hydroxydopamine; BSA, bovine serum albumin; DAU, daunorubicin; DFO, desferrioxamine; DHBA, 2,6-dihydroxybenzaldehyde; DMEM, Dulbecco's modified Eagle's medium; EDTA, ethylenediaminetetraacetic acid; EPI, epinephrine; FAC, ferric ammonium citrate; Fe, iron; IBE, Fe-binding equivalents; ICL670A, deferasirox; L1, deferiprone; NAPQI, *N*-acetyl-*p*-benzoquinone imine; ox6OHDA, 24 h-preoxidized 6-hydroxydopamine; oxEPI, 24 h-preoxidized epinephrine; PDA, photodiode array; ROS, reactive oxygen species; SIH, salicylaldehyde isonicotinoyl hydrazone; *t*-BHP, *tert*-butyl hydroperoxide.

## Supporting information

Cytoprotective effects and stabilities of compounds **1-9** in DMEM medium without BSA supplementation, chromatographic conditions, $^{1}H$ and $^{13}C$ NMR spectra of final compounds **1-9**.

# References

(1) Andrews, N. C., and Schmidt, P. J. (2007) Iron homeostasis. *Annu. Rev. Physiol. 69*, 69-85.

(2) Halliwell, B., and Gutteridge, J. M. C. (2007) *Free radicals in biology and medicine*. 4th ed., Oxford University Press, Oxford ; New York.

(3) Kell, D. B. (2010) Towards a unifying, systems biology understanding of large-scale cellular death and destruction caused by poorly liganded iron: Parkinson's, Huntington's, Alzheimer's, prions, bactericides, chemical toxicology and others as examples. *Arch. Toxicol. 84*, 825-889.

(4) Jomova, K., and Valko, M. (2011) Advances in metal-induced oxidative stress and human disease. *Toxicology 283*, 65-87.

(5) Griendling, K. K., and FitzGerald, G. A. (2003) Oxidative stress and cardiovascular injury: Part I: basic mechanisms and in vivo monitoring of ROS. *Circulation 108*, 1912-1916.

(6) Hennekens, C. H., Buring, J. E., Manson, J. E., Stampfer, M., Rosner, B., Cook, N. R., Belanger, C., LaMotte, F., Gaziano, J. M., Ridker, P. M., Willett, W., and Peto, R. (1996) Lack of effect of long-term supplementation with beta carotene on the incidence of malignant neoplasms and cardiovascular disease. *N. Engl. J. Med. 334*, 1145-1149.

(7) Lee, R., Margaritis, M., Channon, K. M., and Antoniades, C. (2012) Evaluating oxidative stress in human cardiovascular disease: methodological aspects and considerations. *Curr. Med. Chem. 19*, 2504-2520.

(8) Galey, J. B. (2001) Recent advances in the design of iron chelators against oxidative damage. *Mini-Rev. Med. Chem. 1*, 233-242.

(9) Kalinowski, D. S., and Richardson, D. R. (2005) The evolution of iron chelators for the treatment of iron overload disease and cancer. *Pharmacol. Rev. 57*, 547-583.

(10) Powell, L. W., Burt, M. J., Halliday, J. W., and Jazwinska, E. C. (1996) Hemochromatosis: genetics and pathogenesis. *Semin. Liver Dis. 16*, 55-63.

(11) Cohen, A. R., Galanello, R., Pennell, D. J., Cunningham, M. J., and Vichinsky, E. (2004) Thalassemia. *Hematology Am. Soc. Hematol. Educ. Program*, 14-34.

(12) Kwiatkowski, A., Ryckewaert, G., Jissendi Tchofo, P., Moreau, C., Vuillaume, I., Chinnery, P. F., Destee, A., Defebvre, L., and Devos, D. (2012) Long-term improvement under deferiprone in a case of neurodegeneration with brain iron accumulation. *Parkinsonism Relat. Disord. 18*, 110-112.

(13) Salkovic-Petrisic, M., Knezovic, A., Osmanovic-Barilar, J., Smailovic, U., Trkulja, V., Riederer, P., Amit, T., Mandel, S., and Youdim, M. B. (2015) Multi-target iron-chelators improve memory loss in a rat model of sporadic Alzheimer's disease. *Life Sci. 136*, 108-119.

(14) Ward, R. J., Dexter, D. T., and Crichton, R. R. (2015) Neurodegenerative diseases and therapeutic strategies using iron chelators. *J. Trace Elem. Med. Biol. 31*, 267-273.

(15) Reelfs, O., Eggleston, I. M., and Pourzand, C. (2010) Skin protection against UVA-induced iron damage by multiantioxidants and iron chelating drugs/prodrugs. *Curr. Drug. Metab. 11*, 242-249.

(16) Buss, J. L., Torti, F. M., and Torti, S. V. (2003) The role of iron chelation in cancer therapy. *Curr. Med. Chem. 10*, 1021-1034.

(17) Saletta, F., Suryo Rahmanto, Y., Noulsri, E., and Richardson, D. R. (2010) Iron chelator-mediated alterations in gene expression: identification of novel iron-regulated molecules

that are molecular targets of hypoxia-inducible factor-1 alpha and p53. *Mol. Pharmacol. 77*, 443-458.

(18) van Asbeck, B. S., Georgiou, N. A., van der Bruggen, T., Oudshoorn, M., Nottet, H. S., and Marx, J. J. (2001) Anti-HIV effect of iron chelators: different mechanisms involved. *J. Clin. Virol. 20*, 141-147.

(19) Chan, W., Taylor, A. J., Ellims, A. H., Lefkovits, L., Wong, C., Kingwell, B. A., Natoli, A., Croft, K. D., Mori, T., Kaye, D. M., Dart, A. M., and Duffy, S. J. (2012) Effect of iron chelation on myocardial infarct size and oxidative stress in ST-elevation-myocardial infarction. *Circ. Cardiovasc. Interv. 5*, 270-278.

(20) Horackova, M., Ponka, P., and Byczko, Z. (2000) The antioxidant effects of a novel iron chelator salicylaldehyde isonicotinoyl hydrazone in the prevention of H(2)O(2) injury in adult cardiomyocytes. *Cardiovasc. Res. 47*, 529-536.

(21) Simunek, T., Sterba, M., Popelova, O., Adamcova, M., Hrdina, R., and Gersl, V. (2009) Anthracycline-induced cardiotoxicity: Overview of studies examining the roles of oxidative stress and free cellular iron. *Pharmacol. Rep. 61*, 154-171.

(22) Haskova, P., Koubkova, L., Vavrova, A., Mackova, E., Hruskova, K., Kovarikova, P., Vavrova, K., and Simunek, T. (2011) Comparison of various iron chelators used in clinical practice as protecting agents against catecholamine-induced oxidative injury and cardiotoxicity. *Toxicology 289*, 122-131.

(23) Simunek, T., Boer, C., Bouwman, R. A., Vlasblom, R., Versteilen, A. M., Sterba, M., Gersl, V., Hrdina, R., Ponka, P., de Lange, J. J., Paulus, W. J., and Musters, R. J. (2005) SIH--a novel lipophilic iron chelator--protects H9c2 cardiomyoblasts from oxidative stress-induced mitochondrial injury and cell death. *J. Mol. Cell. Cardiol. 39*, 345-354.

(24) Kurz, T., Gustafsson, B., and Brunk, U. T. (2006) Intralysosomal iron chelation protects against oxidative stress-induced cellular damage. *FEBS J. 273*, 3106-3117.

(25) Hašková, P., Kovaříková, P., Koubková, L., Vávrová, A., Macková, E., and Simůnek, T. (2011) Iron chelation with salicylaldehyde isonicotinoyl hydrazone protects against catecholamine autoxidation and cardiotoxicity. *Free Radic. Biol. Med. 50*, 537-549.

(26) Bendova, P., Mackova, E., Haskova, P., Vavrova, A., Jirkovsky, E., Sterba, M., Popelova, O., Kalinowski, D. S., Kovarikova, P., Vavrova, K., Richardson, D. R., and Simunek, T. (2010) Comparison of clinically used and experimental iron chelators for protection against oxidative stress-induced cellular injury. *Chem. Res. Toxicol. 23*, 1105-1114.

(27) Klimtova, I., Simunek, T., Mazurova, Y., Kaplanova, J., Sterba, M., Hrdina, R., Gersl, V., Adamcova, M., and Ponka, P. (2003) A study of potential toxic effects after repeated 10-week administration of a new iron chelator--salicylaldehyde isonicotinoyl hydrazone (SIH) to rabbits. *Acta medica 46*, 163-170.

(28) Sterba, M., Popelová, O., Simůnek, T., Mazurová, Y., Potácová, A., Adamcová, M., Guncová, I., Kaiserová, H., Palicka, V., Ponka, P., and Gersl, V. (2007) Iron chelation-afforded cardioprotection against chronic anthracycline cardiotoxicity: a study of salicylaldehyde isonicotinoyl hydrazone (SIH). *Toxicology 235*, 150-166.

(29) Kovarikova, P., Mrkvickova, Z., and Klimes, J. (2008) Investigation of the stability of aromatic hydrazones in plasma and related biological material. *J. Pharm. Biomed. Anal. 47*, 360-370.

(30) Kovarikova, P., Klimes, J., Sterba, M., Popelova, O., Mokry, M., Gersl, V., and Ponka, P. (2005) Development of high-performance liquid chromatographic determination of salicylaldehyde isonicotinoyl hydrazone in rabbit plasma and application of this method to an in vivo study. *J. Sep. Sci. 28*, 1300-1306.

(31) Edward, J. T., Gauthier, M., Chubb, F. L., and Ponka, P. (1988) Synthesis of new acylhydrazones as iron-chelating compounds. *J. Chem. Eng. Data 33*, 538-540.

(32) Fuchibe, K., Morikawa, T., Ueda, R., Okauchi, T., and Ichikawa, J. (2015) Pinpoint-fluorinated phenanthrene synthesis based on C-F bond activation of difluoroalkenes. *J. Fluor. Chem. 179*, 106-115.

(33) Bieszczad, B., and Barbasiewicz, M. (2015) The Key Role of the Nonchelating Conformation of the Benzylidene Ligand on the Formation and Initiation of Hoveyda-Grubbs Metathesis Catalysts. *Chem. Eur. J. 21*, 10322 - 10325.

(34) Dube, H., Kasumaj, B., Calle, C., Felber, B., Saito, M., Jeschke, G., and Diederich, F. (2009) Probing hydrogen bonding to bound dioxygen in synthetic models for heme proteins: The importance of precise geometry. *Chem. Eur. J. 15*, 125 - 135.

(35) Karabanovich, G., Zemanova, J., Smutny, T., Szekely, R., Sarkan, M., Centarova, I., Vocat, A., Pavkova, I., Conka, P., Nemecek, J., Stolarikova, J., Vejsova, M., Vavrova, K., Klimesova, V., Hrabalek, A., Pavek, P., Cole, S. T., Mikusova, K., and Roh, J. (2016) Development of 3,5-Dinitrobenzylsulfanyl-1,3,4-oxadiazoles and Thiadiazoles as Selective Antitubercular Agents Active Against Replicating and Nonreplicating Mycobacterium tuberculosis. *J. Med. Chem. 59*, 2362-2380.

(36) Hung, M. C., Liao, J. L., Chen, S. A., Chen, S. H., and Su, A. C. (2005) Fine tuning the purity of blue emission from polydioctylfluorene by end-capping with electron-deficient moieties. *J. Am. Chem. Soc. 127*, 14576-14577.

(37) Hruskova, K., Potuckova, E., Hergeselova, T., Liptakova, L., Haskova, P., Mingas, P., Kovarikova, P., Simunek, T., and Vavrova, K. (2016) Aroylhydrazone iron chelators: Tuning antioxidant and antiproliferative properties by hydrazide modifications. *Eur. J. Med. Chem. 120*, 97-110.

(38) Kimes, B. W., and Brandt, B. L. (1976) Properties of a clonal muscle cell line from rat heart. *Exp. Cell. Res. 98*, 367-381.

(39) Jansová, H., Macháček, M., Wang, Q., Hašková, P., Jirkovská, A., Potůčková, E., Kielar, F., Franz, K. J., and Simůnek, T. (2014) Comparison of various iron chelators and prochelators as protective agents against cardiomyocyte oxidative injury. *Free Radic. Biol. Med. 74*, 210-221.

(40) Jansova, H., Bures, J., Machacek, M., Haskova, P., Jirkovska, A., Roh, J., Wang, Q., Franz, K. J., Kovarikova, P., and Simunek, T. (2016) Characterization of cytoprotective and toxic properties of iron chelator SIH, prochelator BSIH and their degradation products. *Toxicology 350*, 15-24.

(41) Potuckova, E., Hruskova, K., Bures, J., Kovarikova, P., Spirkova, I. A., Pravdikova, K., Kolbabova, L., Hergeselova, T., Haskova, P., Jansova, H., Machacek, M., Jirkovska, A., Richardson, V., Lane, D. J. R., Kalinowski, D. S., Richardson, D. R., Vavrova, K., and Simunek, T. (2014) Structure-Activity Relationships of Novel Salicylaldehyde Isonicotinoyl Hydrazone (SIH) Analogs: Iron Chelation, Anti-Oxidant and Cytotoxic Properties. *Plos One 9*, e112059.

(42) Espósito, B. P., Epsztejn, S., Breuer, W., and Cabantchik, Z. I. (2002) A review of fluorescence methods for assessing labile iron in cells and biological fluids. *Anal. Biochem. 304*, 1-18.

(43) Glickstein, H., El, R. B., Link, G., Breuer, W., Konijn, A. M., Hershko, C., Nick, H., and Cabantchik, Z. I. (2006) Action of chelators in iron-loaded cardiac cells: Accessibility to intracellular labile iron and functional consequences. *Blood 108*, 3195-3203.

(44) Mladenka, P., Kalinowski, D. S., Haskova, P., Bobrovova, Z., Hrdina, R., Simunek, T., Nachtigal, P., Semecky, V., Vavrova, J., Holeckova, M., Palicka, V., Mazurova, Y.,

Jansson, P. J., and Richardson, D. R. (2009) The novel iron chelator, 2-pyridylcarboxaldehyde 2-thiophenecarboxyl hydrazone, reduces catecholamine-mediated myocardial toxicity. *Chem. Res. Toxicol. 22*, 208-217.

(45) Richardson, D. R., Sharpe, P. C., Lovejoy, D. B., Senaratne, D., Kalinowski, D. S., Islam, M., and Bernhardt, P. V. (2006) Dipyridyl thiosemicarbazone chelators with potent and selective antitumor activity form iron complexes with redox activity. *J. Med. Chem. 49*, 6510-6521.

(46) Chaston, T. B., Watts, R. N., Yuan, J., and Richardson, D. R. (2004) Potent antitumor activity of novel iron chelators derived from di-2-pyridylketone isonicotinoyl hydrazone involves fenton-derived free radical generation. *Clin. Cancer Res. 10*, 7365-7374.

(47) FDA. (2001) Center for Drug Evaluation and Research (CDER). Bioanalytical method validation guidance for industry. http://www.fda.gov/downloads/Drugs/GuidanceComplianceRegulatoryInformation/Guidances/UCM070107.pdf.

(48) McCallum, M. M., Pawlak, A. J., Shadrick, W. R., Simeonov, A., Jadhav, A., Yasgar, A., Maloney, D. J., and Arnold, L. A. (2014) A fluorescence-based high throughput assay for the determination of small molecule-human serum albumin protein binding. *Anal. Bioanal. Chem. 406*, 1867-1875.

(49) Ràfols, C., Amézqueta, S., Fuguet, E., and Bosch, E. (2018) Molecular interactions between warfarin and human (HSA) or bovine (BSA) serum albumin evaluated by isothermal titration calorimetry (ITC), fluorescence spectrometry (FS) and frontal analysis capillary electrophoresis (FA/CE). *J. Pharm. Biomed. Anal. 150*, 452-459.

(50) Gutteridge, J. M., Richmond, R., and Halliwell, B. (1979) Inhibition of the iron-catalysed formation of hydroxyl radicals from superoxide and of lipid peroxidation by desferrioxamine. *Biochem. J. 184*, 469-472.

(51) Alwood, A. J. (2009) Chapter 79 - Acetaminophen A2 - Silverstein, Deborah C, In *Small Animal Critical Care Medicine* (Hopper, K., Ed.) pp 334-337, W.B. Saunders, Saint Louis.

(52) Dhalla, N. S., Adameova, A., and Kaur, M. (2010) Role of catecholamine oxidation in sudden cardiac death. *Fundam. Clin. Pharmacol. 24*, 539-546.

(53) Costa, V. M., Carvalho, F., Bastos, M. L., Carvalho, R. A., Carvalho, M., and Remiao, F. (2011) Contribution of catecholamine reactive intermediates and oxidative stress to the pathologic features of heart diseases. *Curr. Med. Chem. 18*, 2272-2314.

(54) Thomas, C. E., and Aust, S. D. (1986) Reductive release of iron from ferritin by cation free radicals of paraquat and other bipyridyls. *J. Biol. Chem. 261*, 13064-13070.

(55) Keizer, H. G., Pinedo, H. M., Schuurhuis, G. J., and Joenje, H. (1990) Doxorubicin (adriamycin): a critical review of free radical-dependent mechanisms of cytotoxicity. *Pharmacol. Ther. 47*, 219-231.

(56) Richardson, D. R., and Ponka, P. (1997) The molecular mechanisms of the metabolism and transport of iron in normal and neoplastic cells. *Biochim. Biophys. Acta-Rev. Biomembr. 1331*, 1-40.

(57) Potuckova, E., Jansova, H., Machacek, M., Vavrova, A., Haskova, P., Tichotova, L., Richardson, V., Kalinowski, D. S., Richardson, D. R., and Simunek, T. (2014) Quantitative analysis of the anti-proliferative activity of combinations of selected iron-chelating agents and clinically used anti-neoplastic drugs. *PLoS One 9*, e88754.

(58) Simunek, T., Sterba, M., Popelova, O., Kaiserova, H., Adamcova, M., Hroch, M., Haskova, P., Ponka, P., and Gersl, V. (2008) Anthracycline toxicity to cardiomyocytes or cancer cells

is differently affected by iron chelation with salicylaldehyde isonicotinoyl hydrazone. *Br. J. Pharmacol. 155*, 138-148.

(59) Hatcher, H. C., Singh, R. N., Torti, F. M., and Torti, S. V. (2009) Synthetic and natural iron chelators: therapeutic potential and clinical use. *Future Med. Chem. 1*, 1643-1670.

(60) Kremastinos, D. T., and Farmakis, D. (2011) Iron overload cardiomyopathy in clinical practice. *Circulation 124*, 2253-2263.

# Tables

**Table 1.** Cytotoxic and cytoprotective effects of the novel SIH derivatives in H9c2 cells expressed as $TC_{50}$ and $EC_{50}$, respectively.

| | CLogP† | $TC_{50}$ [μM] (after 72 h) | $EC_{50}$ [μM] (after 24 h) | Relative protection * | |
|---|---|---|---|---|---|
| | | | | at 30 μM | at 100 μM |
| **SIH** | 2.07 | **15.3 ± 2.2** | **N/A** | **26.4 ± 6.5** | **34.7 ± 9.4** |
| **DHBA** | 1.7 | 230.8 ± 31.2 | N/A | 1.0 ± 0.4 | 0.4 ± 0.2 |
| **1** | 2.18 | 20.1 ± 1.3 | 40.7 ± 4.2 | **58.8 ± 5.3** | **65.2 ± 6.7** |
| **2** | 2.18 | 22.5 ± 5.7 | 64.3 ± 2.1 | **46.3 ± 4.1** | **53.1 ± 1.5** |
| **3** | 3.34 | 21.0 ± 2.6 | 38.5 ± 7.0 | **55.5 ± 9.3** | **63.6 ± 4.8** |
| **4** | 3.84 | 13.2 ± 1.5 | 125.6 ± 8.0 | 35.8 ± 8.1 | 45.2 ± 7.1 |
| **5** (JK-31) | 4.15 | **15.2 ± 3.5** | **18.2 ± 3.8** | **65.5 ± 5.4** | **69.5 ± 6.5** |
| **6** | 4.15 | 6.5 ± 0.8 | N/A | 25.5 ± 4.2 | 35.2 ± 5.2 |
| **7** | 4.30 | 11.2 ± 1.4 | N/A | **47.4 ± 9.8** | **49.7 ± 7.6** |
| **8** | 1.67 | 36.4 ± 6.4 | N/A | 21.3 ± 9.3 | 34.3 ± 4.6 |
| **9** | 3.95 | 87.2 ± 9.6 | N/A | 1.0 ± 0.6 | 13.6 ± 9.2 |

* Cytoprotective effects of the studied compounds at 30 μM and 100 μM concentrations against $H_2O_2$-induced damage (complete viability loss) toward H9c2 cells expressed as a percentage of viability compared to control (100 %).

† CLogP values were calculated using ChemDraw Professional 15.

N/A –value not within the studied concentration range.

**Table 2.** Antiproliferative effects of SIH derivatives.

| | **MCF-7** $IC_{50}$ **[μM]** | **HeLa** $IC_{50}$ **[μM]** |
|---|---|---|
| **SIH** | 21.9 ± 4.8 | 56.9 ± 6.7 |
| **DHBA** | 285.3 ± 13.5 | > 300 |
| **1** | 53.4 ± 3.9 | 69.7 ± 3.2 |
| **2** | 59.4 ± 8.4 | 78.2 ± 13.8 |
| **3** | 26.1 ± 3.7 | 62.8 ± 5.9 |
| **4** | 14.0 ± 2.2 | 25.0 ± 12.2 |
| **5** (JK-31) | **5.7 ± 1.2** | **18.7 ± 1.2** |
| **6** | 20.4 ± 5.9 | 56.0 ± 17.6 |
| **7** | **5.2 ± 1.1** | **21.4 ± 5.0** |
| **8** | 50.9 ± 3.8 | 109.1 ± 16.5 |
| **9** | 40.5 ± 2.7 | 84.0 ± 11.5 |

# Schemes

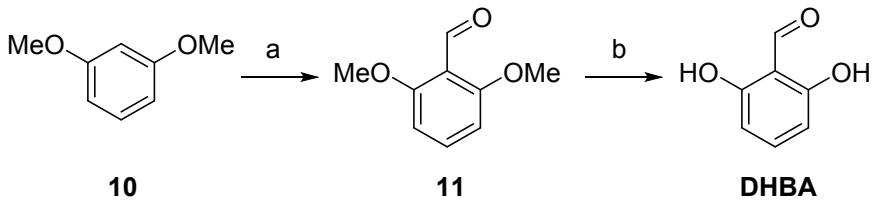


**Scheme 1.** Synthesis of 2,6-dihydroxybenzaldehye (DHBA). Reagents and conditions: (a) 1. n-BuLi, THF, -5 °C – rt, 50 min; 2. DMF, 0 °C, 1 h, 87%; (b) $AlCl_3$, $CH_2Cl_2$, rt, 24 h, 62%.

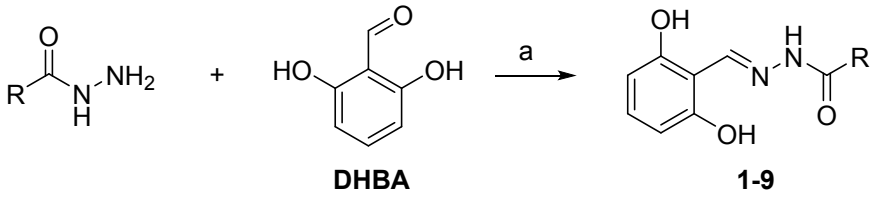


**Scheme 2.** Synthesis of final 2,6-dihydroxybenzaldehyde aroylhydrazones **1-8** and alkanoylhydrazone **9**. Reagents and conditions: (a) 3-5 drops of $CH_3COOH$, EtOH (96%), reflux, 2-24 h, 53-99%.

# Figures

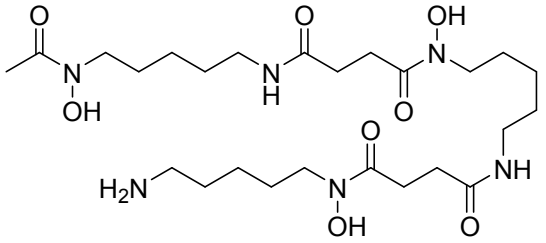


desferrioxamine (DFO)

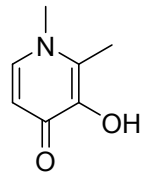


deferiprone (L1)

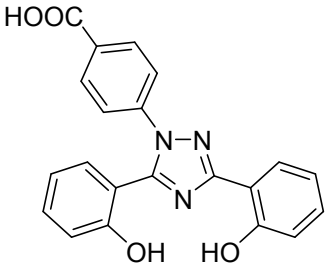


deferasirox (ICL670A)

**Fig. 1. S**tructures of Fe chelators currently in clinical practice

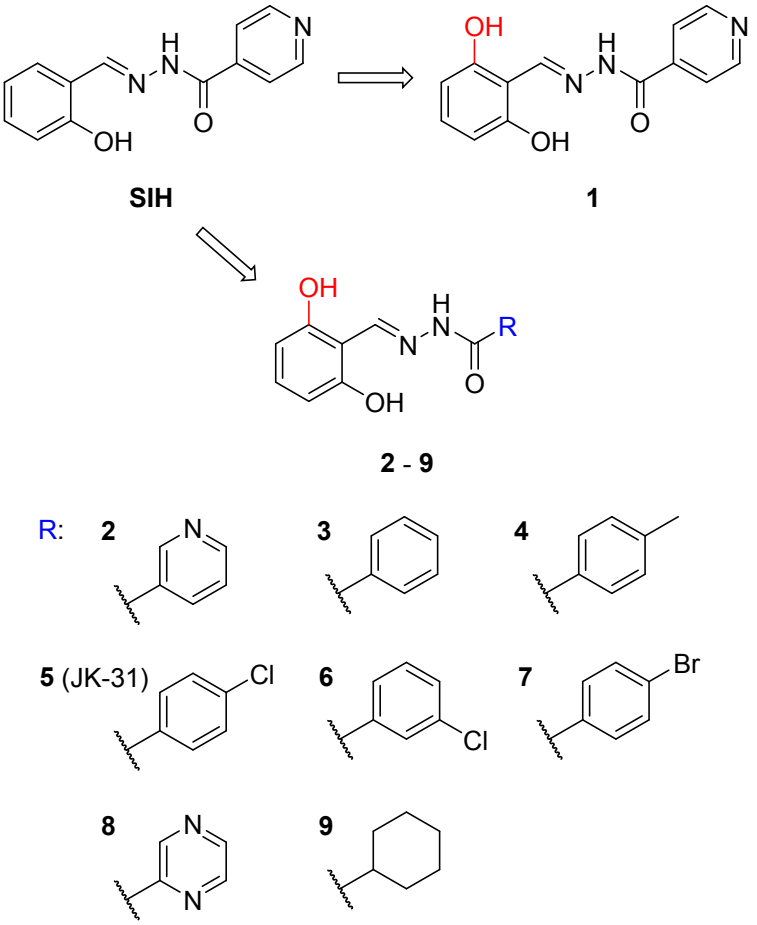


**Fig. 2** Structures of the parent chelator SIH and its analogues **1-9** studied in this work

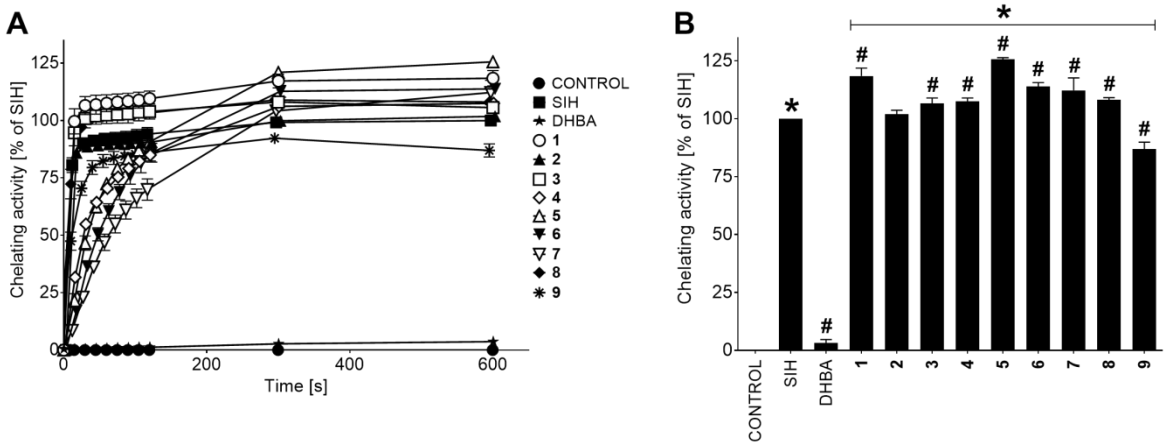


**Fig. 3** Fe-chelating efficiencies of the studied compounds in solution at a concentration of 100 μM. Chelating activities of the tested compounds were examined by the determination of Fe displacement from its complex with calcein in a buffered solution (pH = 7.2). The efficiency of the chelation is expressed relative to SIH at t = 10 min (100 %). (A) The time-profile of the fluorescence intensity monitored over 10 min after tested compounds were mixed with the Fe-calcein complex. (B) Mean changes in fluorescence intensity after the 10 min incubation with the studied compounds. Data are presented as the means ± SD; n = 4; statistical significance (ANOVA, $p \leq 0.05$): * compared to the control; # compared to SIH.

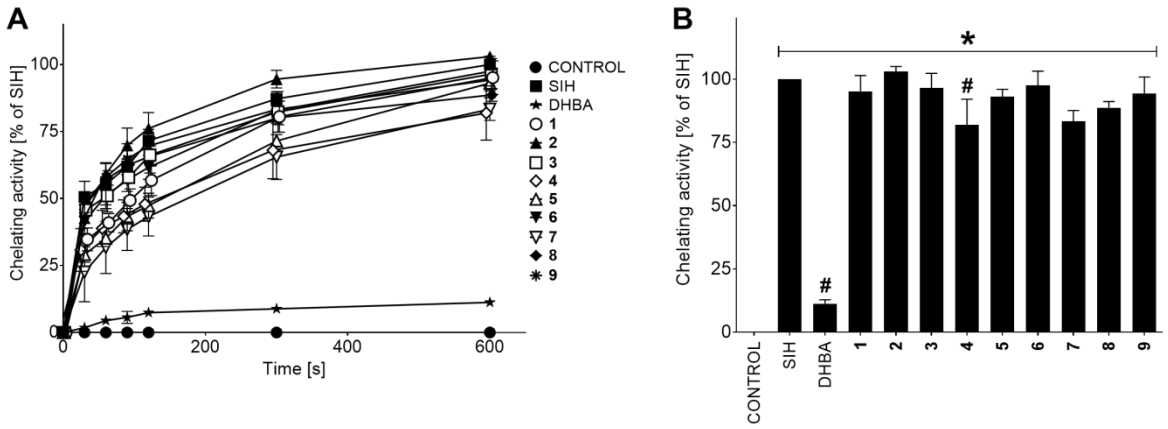


**Fig. 4** Potential of the tested compounds to bind intracellular Fe at a concentration of 100 μM. The fluorescence increase after displacement of the labile Fe from its complex with intracellularly trapped calcein in H9c2 cardiomyoblast cells after the extracellular application of the studied compounds. (A) The time-profile of the fluorescence intensity. (B) Mean fluorescence intensity changes after the 10 min incubation with the examined chelators. The efficiency of the chelation is expressed relative to SIH at t = 10 min (100 %). The data are presented as the means ± SD; n = 4; statistical significance (ANOVA, $p \leq 0.05$): * compared to the control; # compared to SIH.

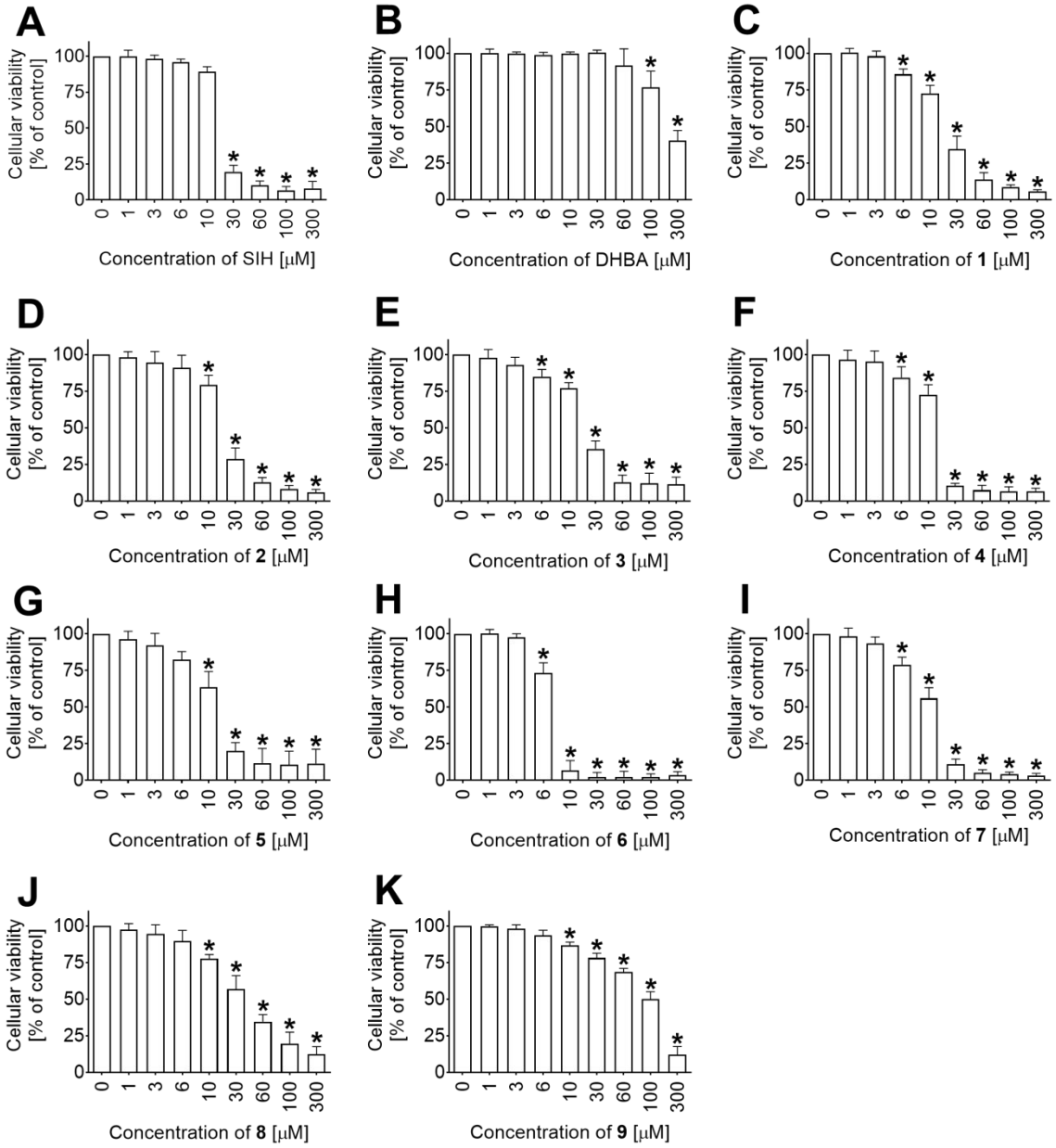


**Fig. 5** Inherent toxicities of the tested compounds SIH (A), DHBA (B), compound **1** (C), **2** (D), **3** (E), **4** (F), **5** (G), **6** (H), **7** (I), **8** (J) and **9** (K). H9c2 cardiomyoblast cells were incubated with the tested chelators for 72 h. The cellular viabilities are expressed relative to the untreated control (100 %). Data are presented as the means ± SD; n = 3-4; statistical significance (ANOVA, $p \leq 0.05$): * compared to the control.

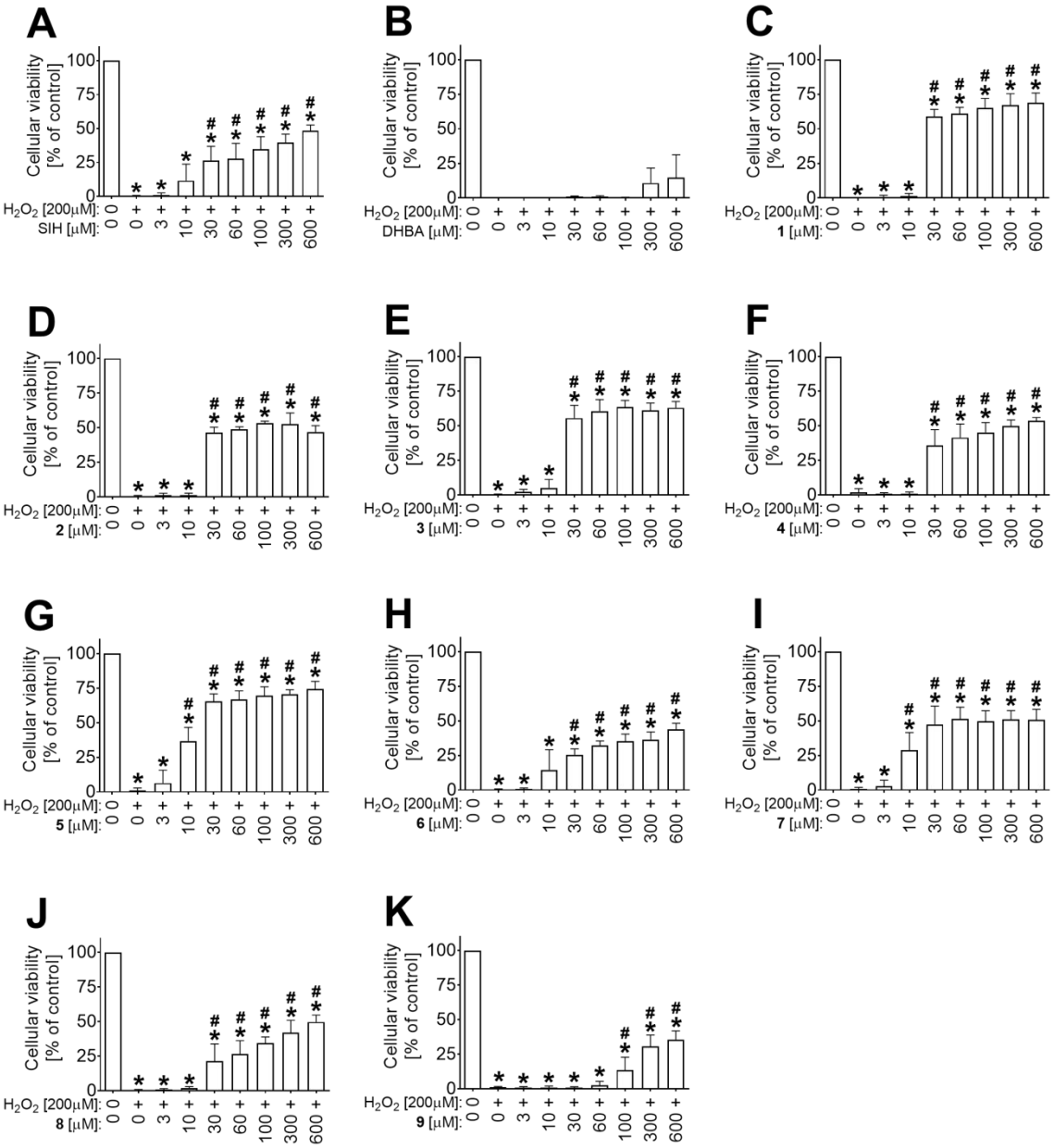


**Fig. 6** Cytoprotective properties of SIH (A), DHBA (B), **1** (C), **2** (D), **3** (E), **4** (F), **5** (G), **6** (H), **7** (I), **8** (J) and **9** (K) against toxicity induced by 24 h of exposure of H9c2 cardiomyoblast cells to $H_2O_2$ (200 μM). The cellular viabilities and expressed relative to the untreated control (100 %).

The data are presented as the means ± SD; n = 3-4; statistical significance (ANOVA, $p \leq 0.05$):

* compared to the control; # compared to the $H_2O_2$-treated group.

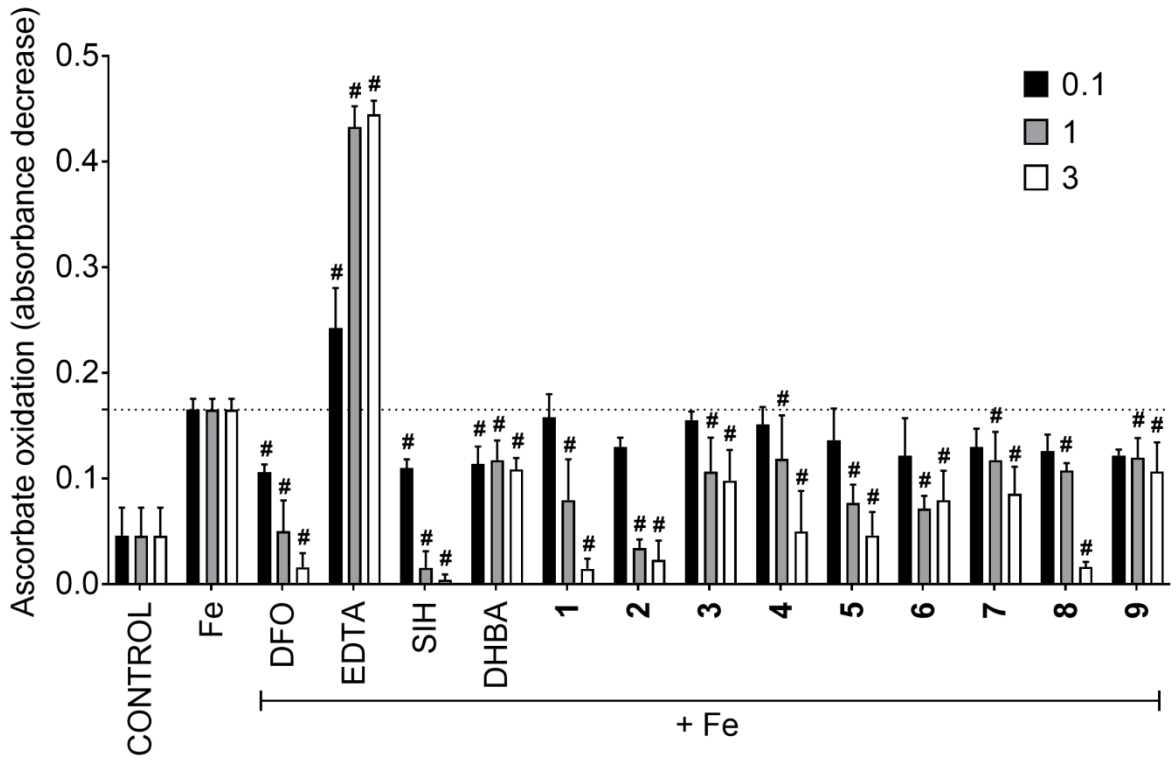


**Fig. 7** Influence of SIH and its novel analogues **1-9** on the Fe-mediated oxidation of ascorbate in a buffered solution (pH 7.4). EDTA and DFO were used as the positive and negative control chelators, respectively. The studied compounds were evaluated at IBE values of 0.1 (excess Fe), 1 (complexes of the Fe with the studied compounds with a fully saturated coordination sphere) and 3 (excess of the studied compound). The results are expressed as absorbance decrease after 30 min of incubation ($T_{10} - T_{40}$). The data are presented as the means ± SD; $n \geq 3$; statistical significance (ANOVA, $p \leq 0.05$): # compared to the Fe-treated group.

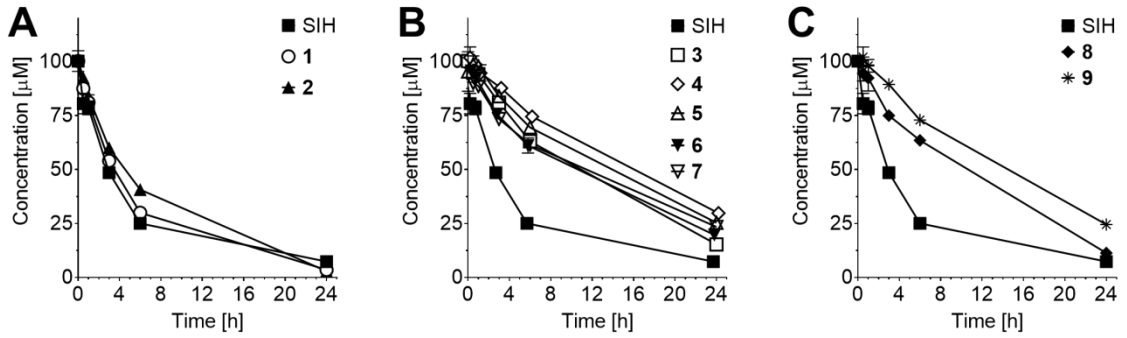


**Fig. 8** Stabilities of SIH and its derivatives **1**-**9** in DMEM supplemented with BSA. The studied compounds were incubated (37 °C) at initial concentrations of 100 μM for 24 h in DMEM supplemented with BSA. Their concentrations at selected time intervals were assessed using HPLC analysis. A – Stability of SIH and its closest derivatives (compounds **1** and **2**) bearing (iso)nicotinoyl groups; B – Stability of SIH and its unsubstituted and monosubstituted benzohydrazone analogues (compound **3**, **4**, **5**, **6** and **7**), which are more lipophilic; C – Stability of SIH and studied compounds **8** and **9**. The data are presented as the means ± SD; n = 3.

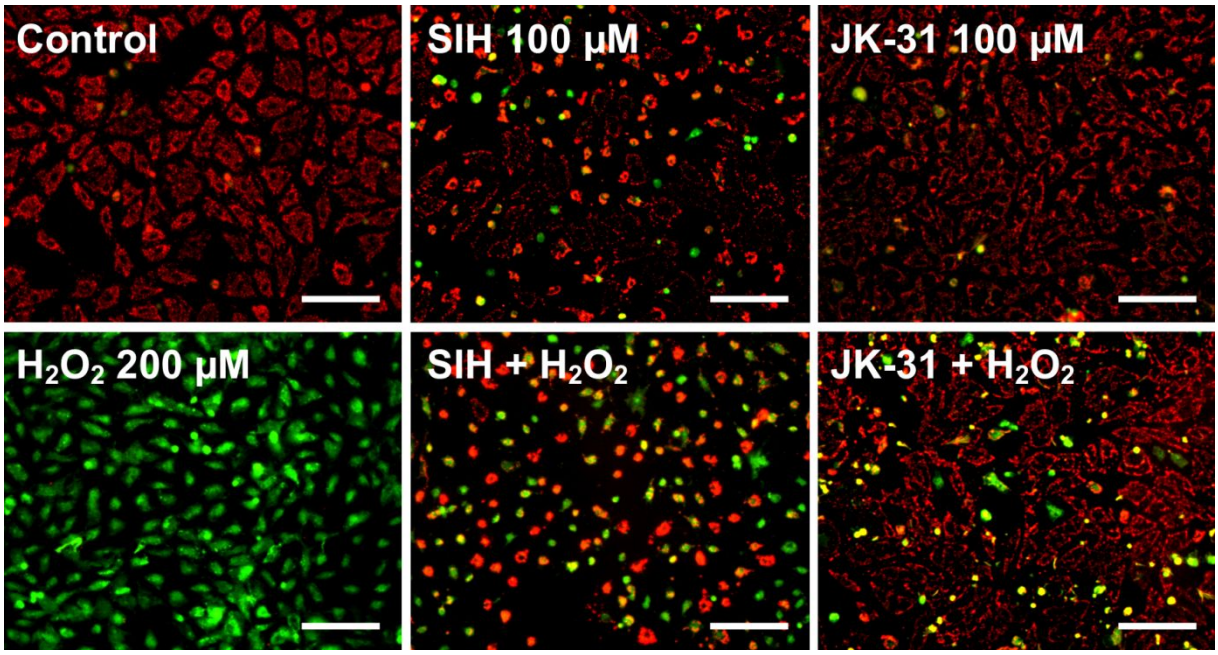


**Fig. 9** Mitochondrial inner membrane potentials ($\Delta\Psi_m$ values) were studied using the fluorescence microscopy. H9c2 cardiomyoblast cells were incubated for 24 h with SIH, JK-31 and $H_2O_2$ (alone or in combinations) and then stained with the JC-1 probe. Punctate or rod-shaped red emission of JC-1 indicates actively respiring mitochondria, whereas diffuse green fluorescence indicates mitochondrial depolarization. Lack of fluorescence indicates probe release from necrotic or secondary apoptotic cells. Upper photographs show the own toxicities of the assayed chelators (all 100 µM) , the lower photographs show the protective effects of these compounds against the $\Delta\Psi_m$ dissipation induced by $H_2O_2$ (200 µM) . Scale bars represent 200 µm.

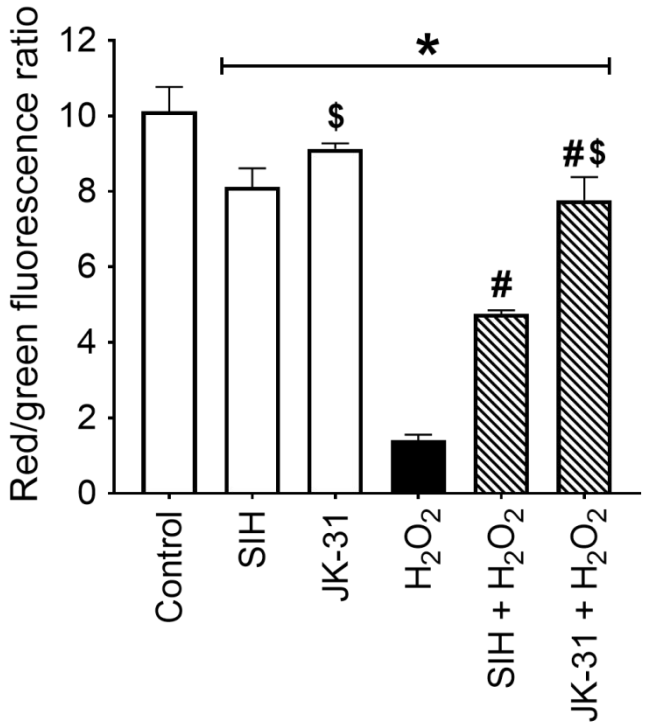


**Fig. 10** The mitochondrial inner membrane potentials ($\Delta\Psi_m$) expressed as the ratio of the red and green fluorescence intensities of the JC-1 probe. H9c2 cardiomyoblast cells were incubated for 24 h with SIH or JK-31 (100 μM) and $H_2O_2$ (200 μM) and then stained with the JC-1 probe. The data are presented as the means ± SD; n = 4; statistical significance (ANOVA, $p \leq 0.05$): * compared to the control group; # compared to the $H_2O_2$-treated group; $ compared to the appropriate SIH-treated group.

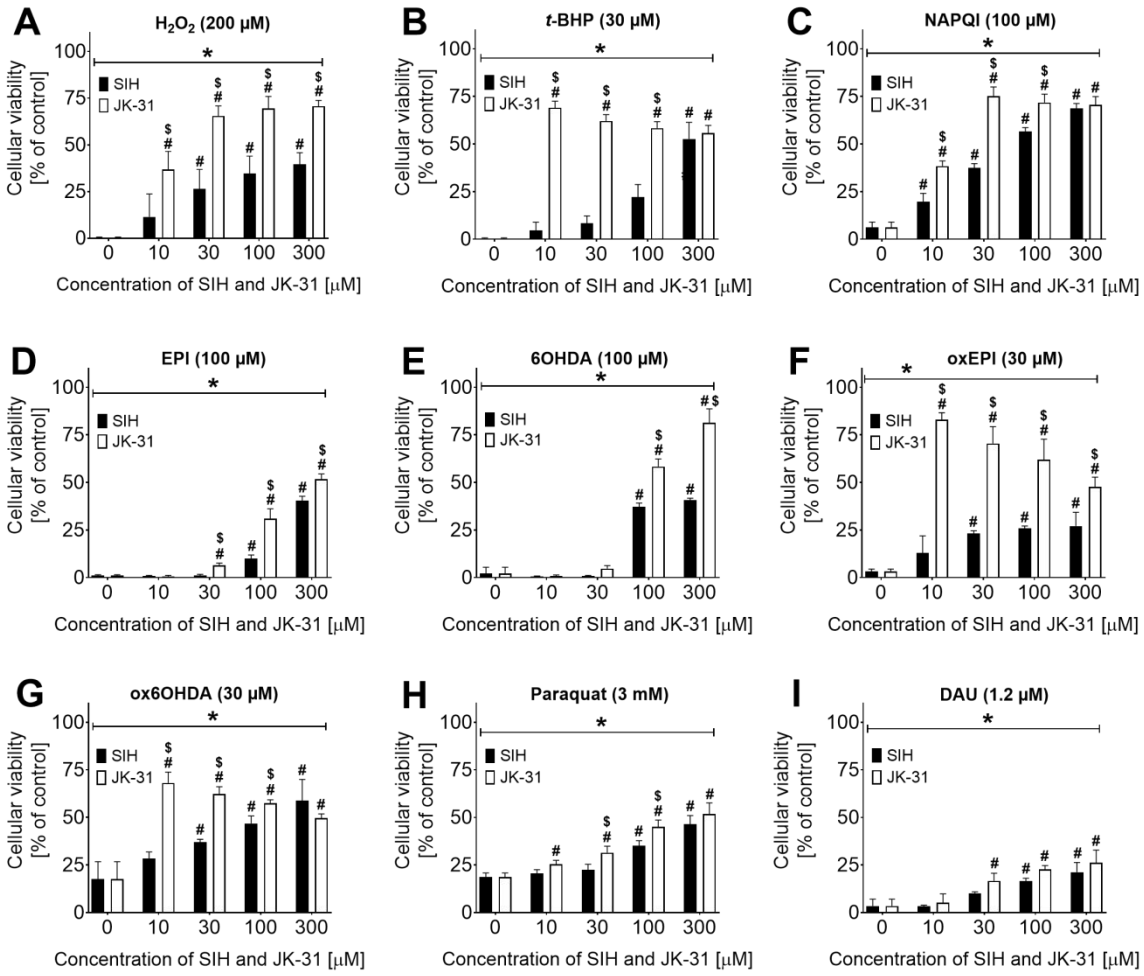


**Fig. 11** Protective effects of SIH and JK-31 against the cellular toxicity induced in H9c2 cells by 24 h of exposure to various pro-oxidants (A - hydrogen peroxide ($H_2O_2$; 200 μM), B - *tert*-butyl hydroperoxide (*t*-BHP; 30 μM), C - *N*-acetyl-*p*-benzoquinone imine (NAPQI; 100 μM), D – epinephrine (EPI; 100 μM), E - 6-hydroxydopamine (6OHDA; 100 μM), F – 24 h-preoxidized epinephrine (oxEPI; 30 μM), G - 24 h-preoxidized 6-hydroxydopamine (ox6OHDA; 30 μM), H - paraquat (3 mM) and I – daunorubicin (DAU; 1.2 μM)). The cellular viabilities are expressed as a percentage relative to the untreated control (100 %). The data are presented as the means ± SD; n = 4; statistical significance (ANOVA, $p \leq 0.05$): * compared to the control; # compared to the pro-oxidant-treated group; $ compared to the appropriate SIH-treated group.

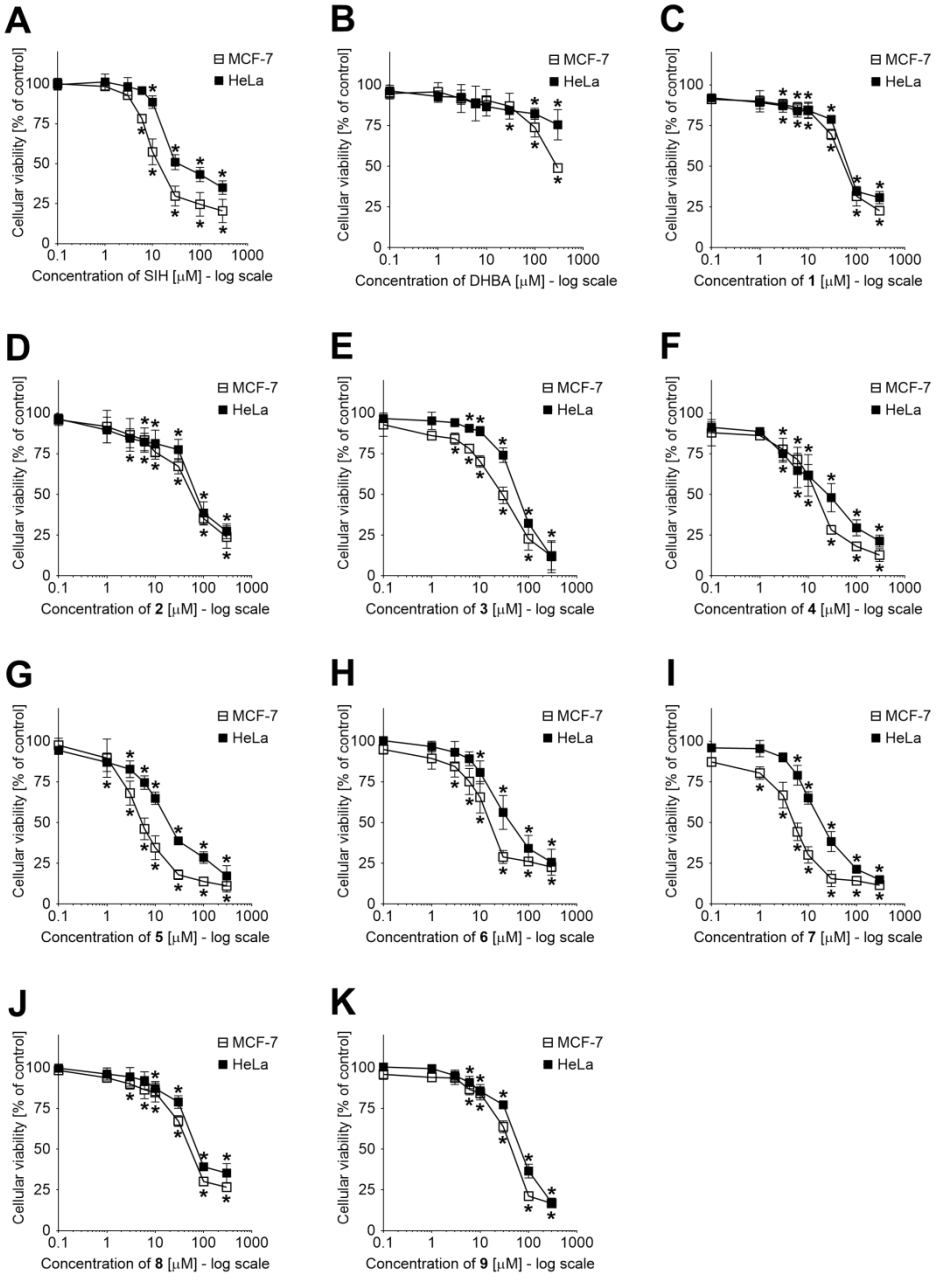


**Fig. 12** Antiproliferative effects of tested compounds SIH (A), DHBA (B), **1** (C), **2** (D), **3** (E), **4** (F), **5** (G), **6** (H), **7** (I), **8** (J) and **9** (K). MCF-7 (□) and HeLa (■) cells were incubated with the studied compounds for 72 h. The cellular viabilities are expressed relative to the untreated control (100 %). The data are presented as the means ± SD; n = 3-4; statistical significance (ANOVA, $p \leq 0.05$): * compared to the control.